Mehran University Research Journal of Engineering and Technology

https://doi.org/10.22581/muet1982.0379

2026, 45(1) 88-114

Comprehensive 4Es (Energy, Exergy, Economic, Environmental) Analyses of Dedicated Mechanical Subcooled Vapour Compression Refrigeration Systems Using Low-GWP Refrigerants as R134a substitutes

Jeremiah Odion Akhimien[a,*], Iyenagbe Benjamin Ugheoke[a], Wilfred Onoshiorena Ikalumhe[a], Nihad S. Achekuogene[a], Hope O. Imoedemhe[b], Haruna Suleman Ogweda[a]

[a]*Department of Mechanical Engineering, Edo University Iyamho, Edo State, Nigeria.*
[b]*Department of Electrical/Electronic Engineering, Edo University Iyamho, Edo State, Nigeria.*
[*] Corresponding author: Jeremiah Odion Akhimien, Email: *akhimien.jeremiah@edouniversity.edu.ng*

Received:03 June 2025, Revised: 05 December 2025, Accepted: 24 December 2025, Published: 01 January 2026

K E Y W O R D S

Coefficient of performance
Exergy Efficiency
TEWI Analysis
Refrigerant Safety
Annual Total Cost Rate
Low GWP Refrigerants Alternatives

A B S T R A C T

With increasing restrictions on high GWP refrigerants in refrigeration system, th transition to efficient, climate-friendly alternatives has become necessary. Some efficier low GWP options fall within the A2/A2L flammability class, necessitating stric adherence to safety standards, introducing additional design and cost implications Despite these challenges, integrated assessments that simultaneously addres performance, environmental impact, safety requirements, and economic viability in dedicated mechanical subcooling refrigeration system (DMS-VCRS) remain scarce.

This study presents a comprehensive parametric evaluation of seven R134A substitute under the DMS-VCRS framework using 4Es (Energy, Exergy, Economic, Environmental analysis. It includes TEWI-based environmental analysis and safety-economi assessments for A2/A2L refrigerants. The R134a substitute refrigerants that wer examined in this work include R1234ze(E), R1234yf, R440A, R450A, R513A, R515A and R152A. The model of the DMS-VCRS was carried out using STEAG Ebsilo Professional software with REFPROP 9.1 thermophysical property correlation. Th model validation demonstrated excellent agreement with the literature (RMSE = 0.0334 MAPE < 3%, R^2 > 0.997).

Parametric studies investigated the influence of condenser temperatures, evaporato temperatures, degrees of subcooling, degrees of superheating, and refrigerant mass-flov ratios on thermodynamics, economics, and environmental impacts performance. R152A and R440A performed better than R134A, achieving a 7% increase in COP, a 6% increas in exergy efficiency, and a 13–22% reduction in Total Equivalent Warming Impac (TEWI) compared to R134A. Reliability-bounded operating ranges for subcoolin degrees (22–39.5 °C) and superheating degrees (1.5–37.5 °C), along with othe parameters, yielded optimal conditions at 34–37 °C condenser 1 temperature, −4 °(evaporator temperature, and 27.3–32.5 °C and 20–25 °C subcooling and superheating respectively. The performance of 4Es was consistently and mildly impacted by variation in superheating and subcooling degrees. While indirect emissions from powe consumption show a total TEWI (>85%). Their economic competitiveness i demonstrated by the fact that R152A and R440A had the lowest Annual Total Cost Rat (ATCR) (≈5% below R134a) and Total System Cost (TCR-SYS), which was roughly 9% higher than R134a but 12% lower than R1234yf. Although R152A and R440A are mildl flammable (A2), safe operation can be ensured under the IEC 60335-2-89 guidelin through charge limitation, leak detection, and ventilation.

1. Introduction

Conventional Vapour compression refrigeration systems (VCRS) continue to dominate industrial and commercial cooling but they are known for substantial energy consumption. R134a has been used as a standard working fluid for decades; its high global warming potential poses serious environmental concerns. Extensive VCRS deployment contributes substantially to global energy consumption and greenhouse gas emissions [1–3]. The 2016 Kigali Amendment mandates gradual reduction HFCs, including R134a [4, 5]. This regulatory framework necessitated industry adoption of low-GWP refrigerants with improved refrigeration system configurations such as mechanical subcooling [6].

Recent studies have explored multiple low GWP alternatives for R134a, with particular focus on R1234yf and R1234ze(E), due to their ultra-low GWP (below 10) and comparable operating pressure to R134A, as well as several blended refrigerants which include: R513A, R515A, R440A, and R450A. Most alternatives achieve GWP values below 150, though R450A, R513A, and R515A exceed this benchmark [7]. The studied refrigerants have been shown to have similar thermophysical properties to R134A [8, 9], but they show a lower coefficient of performance (COP) and volumetric cooling capacity (VCC) compared to R134A [10, 11]. Aprea et al. [8] reported a 5-10% reduction in COP for R1234yf compared to R134A. While Nawaz et al. [12] reported an acceptable energy performance for R1234ze(E) despite lower VCC. Blended refrigerants (R-440A, R-450A, R-513A, R-515A) offer similar performance characteristics with GWP values below 630 [13]. Bolaji [14] observed COP improvements of 14% and 5% for R440A and R450A, respectively. Li [15] identified R513A, R515B, and R516A as practical substitutes for R134A. They noted that R516A show superior performance among the three evaluated refrigerants but requires a safety protocol due to its A2L classification, while R515B demand significant compressor modifications. Kizilboga et al. [23] examined low GWP refrigerants in automotive applications. They found that R152A, among the evaluated refrigerants, exhibited the lowest total exergy destruction despite A2 classification. Deymi-Dashtebayaz et al. [22] applied second law analysis to optimise refrigeration configurations, focusing on exergy-based performance evaluation of low GWP refrigerants. Their work identified optimal conditions maximising exergy efficiency while minimising irreversibilities, establishing a framework for sustainable design.

Dedicated mechanical subcooling (DMS) has gained research interest for performance improvement. The application of DMS helps to increase refrigeration effect while reducing compressor work, improving COP and exergy efficiency [16–18]. Studies report 8-15% COP gains [11, 18, 19]. Component-level exergy analysis in DMS-VCRS reveals reduced irreversibility's, particularly in evaporators and expansion devices. Wu and Wang [20] emphasised that expansion valve exergy destruction decreases significantly with mechanical subcooling. Solanki et al. [18] and Zheng et al. [21] reported reduced compressor work and overall exergy destruction.

Financial analyses using Net present Value (NPV), life cycle cost (LCC), and payback metrics indicate subcooling modifications could achieve 2–4 years cost recovery [27]. Research confirms that DMS integration improves not only efficiency but also maintains economic viability [17, 18, 28]. Existing DMS-VCRS studies, particularly with R134a, focus predominantly on thermodynamic performance or 3Es analyses [18, 19, 46]. These studies have advanced DMS understanding with high GWP refrigerants, which provide limited insight into low GWP performance under identical conditions. Studies have examined low GWP refrigerants or DMS separately; a comprehensive 4Es evaluation combining both remains rare.

TEWI assessments show electricity consumption dominates environmental impact [24]. Kumar et al. [25] demonstrated how grid carbon intensity critically influences indirect emission significance in TEWI calculations, emphasising energy efficiency's importance beyond refrigerant GWP in refrigerant selection and system optimisation. Refrigerant selection has been shown to have a critical influence on environmental sustainability [4, 29]. Environmental criteria must be integrated with thermodynamic and economic factors in refrigeration assessment for system sustainability. Kayes et al. [26] applied a 4Es (energy, exergy, environmental, economic) analysis to CO_2 systems, demonstrating that environmental factors can shift thermodynamic optimisation points.

Literature rarely integrates A2/A2L safety requirements—charge limits, ventilation, leak detection, and compliance with IEC 60335-2-89, ISO 5149, and EN 378—into economic frameworks. This safety cost remains inadequately quantified in economic assessment. Some promising alternatives (R152A, R440A, R1234yf, R1234ze(E)) carry A2/A2L classifications, which demand safety-related design modifications.

This work addresses these gaps through 4Es (energy, exergy, economic, environmental) assessment of DMS-VCRS with seven low GWP refrigerants as R134a substitutes, integrating TEWI analysis and safety-compliant economics. The aim of this study is achieved through regulatory-aligned refrigerant selection guidance that balances efficiency, safety, cost, and environmental sustainability.

2. Materials And Methods

This study presents a comprehensive evaluation of seven R134A substitutes under the DMS-VCRS framework, which includes an integrated condenser cooling fan. Seven low-GWP refrigerants, including R1234yf, R1234ze(E), R440A, R450A, R513A, R515A, and R152A, were analysed for being substitutes for the R134a refrigerant in a study. It investigates the impact of variations in the temperatures of the condenser and evaporator, superheating degree of the subcooling circuit, subcooling degree, and the mass flow ratio of the working fluid on the performance of the system, namely, annual total plant cost rate (ATCR), system total cost rate (TCR-SYS), TEWI, COP and exergy efficiency.

2.1 System Description

Figure 2(a–c) shows the DMS-VCRS schematic together with the corresponding pressure-enthalpy (p-h) and temperature-entropy (T-s) diagrams. The primary DMS-VCRS circuit includes a compressor, condenser, expansion valve, and evaporator, which operate in a closed-loop setup (see Fig. 2a). The auxiliary DMS-VCRS circuit is thermally linked to the primary circuit through a sub cooler. Acting as an evaporator for the auxiliary loop, the sub cooler lowers the primary circuit refrigerant temperature below its saturation point at the condenser pressure. This design improves the refrigerating effect without increasing the compressor work. Air cooling for both condensers is provided by the forced-draft fans.

2.2 Steag Ebsilon Modeling And Simulation Of The Refrigeration Cycle

The 4Es (energy, exergy, economic, and environmental) assessment of a DMS-VCRS was performed using STEAG Ebsilon Professional (v16.0) software. This platform offers good capability for steady-state and quasi-dynamic simulations with accurate heat and mass balance calculations. Although originally developed for power generation applications, the software can be adapted effectively to detailed refrigeration system modelling through its extensive component library, integrated material databases, and kernel scripting features [30].

Thermophysical property calculations use REFPROP 9.1 correlations, which guarantee precise refrigerant and air property computation across all operating conditions [31]. The software allows user-defined equations for exergy, economic, and Total Equivalent Warming Impact (TEWI) calculations through its integrated kernel-scripting feature.

2.2.1 Model Construction Methodology

The DMS-VCRS model was developed using Ebsilon's component library as follows (Fig. 1):

- Main Refrigeration Loop: Compressor (Comp. 24 + 29), Condenser (Comp. 7), Expansion Valve (Comp. 14), and Evaporator (Comp. 26).
- Subcooling Loop: Secondary Compressor (Comp. 24 + 29), Condenser (Comp. 7), Expansion Valve (Comp. 14), and Sub cooler (Comp. 26).
- Auxiliary Systems: Centrifugal Fans (Comp. 24 + 29), control elements (Comp. 39), and kernel scripts for control integration and system performance metrics calculation.

Boundary conditions and convergence criteria were defined as: convergence tolerance = 1×10^{-7}, and maximum iterations = 900.

2.3 Mathematical Modelling

2.3.1 Energy and Exergy Analysis

A thermodynamic and exergetic model of the DMS-VCRS was developed based on established formulations from literature to evaluate system performance and cost characteristics (see Table 3). The following assumptions were applied to ensure model simplicity and computational stability:

1. Pressure drops of 2% for the main loop and 1% for the DMS loop components. Heat losses of 0.5%
2. Kinetic and potential energy effects are neglected.
3. All components operate under steady-state conditions.
4. Expansion in both main and subcooling loops is isenthalpic.
5. The refrigeration capacity is fixed at 15 kW to maintain safe refrigerant charge limits (<1.2 kg) for A2 and A2L refrigerants at the designed 40 °C condenser temperature.
6. Inlet air temperatures for the condenser and evaporator fans are constant at 25 °C.

Table 2 presents the principal input parameters and governing equations derived from the first and second laws of thermodynamics used for system analysis.

The compressor-driven refrigerant mass flow rate (m˙_R1) in the main cycle is determined through a heat balance analysis of the evaporator using Equations (1).

$$\dot{m}_{R1} = \frac{\dot{Q}_{Evap}}{(h_1 - h_5)} = \frac{\dot{Q}_{6-7}}{(h_1 - h_5)} \quad (1)$$

The compressor-driven refrigerant mass flow rate ($\dot{m}_{R2}$) in the subcooling cycle is determined through a heat balance analysis of the subcooler using Equations (2).

$$\dot{m}_{R2} = \frac{\dot{m}_{R1}(h_4 - h_3)}{(h_{10} - h_{13})} \quad (2)$$

The Volumetric Cooling Capacity ($\dot{Q}_{v,CS}$, kJm $^{-3}$) represents the refrigerating effect per unit volume of refrigerant at the compressor suction inlet. This parameter is calculated from the specific refrigerating effect (Q_{evap}, kJkg −1) and the vapour density at the compressor suction point [43].

$$\dot{Q}_{v,CS} = \left(\frac{\dot{Q}_{Evap}}{\dot{m}_{R1} \times v_1} + \frac{(h_{10} - h_{13})}{v_{10}}\right) \quad (3)$$

Where v_1 and v_{10} is the suction specific volume at the compressor's inlet at the main and subcooling cycle.

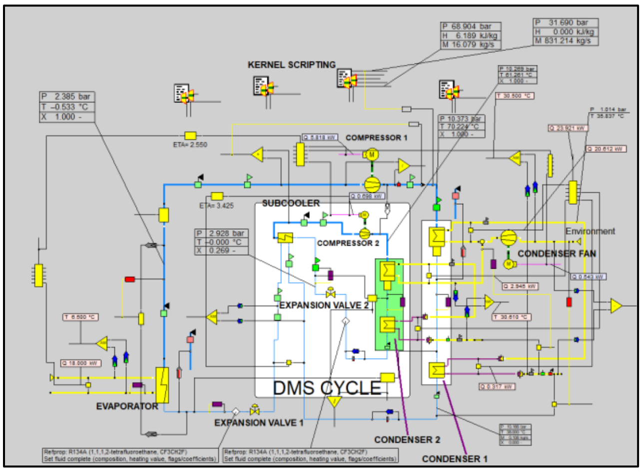

Fig. 1. DMS-VCRS modelled in the STEAG Ebsilon environment.

Table 1

Properties of Selected Refrigerants [11], [32]–[35]

Properties	Refrigerants							
	R134A	R1234ze	R1234yf	R440A	R450A	R513A	R515A	R152A
Global Warming Potential (GWP)	1430	7	4	144	537	631	393	124
Safety Class*	A1	A2L	A2L	A2L	A1	A1	A1	A2
Boiling Point (°C)	-26.1	-19.0	-29.5	-25.5	-23.1	-29.2	-19.2	-24.0
Critical Temp. (°C)	101.1	109.4	94.7	103.5	104.4	96.5	108.7	113.3
Critical Press. (kPa)	4059	3635	3382	4003	3820	3858	3571	4520
Liquid Density @25°C (kg/m³)	1206	1163	1091	1097	1175.1	1134	1181	899
Vapour Density @25°C (kg/m³)	32.35	30.12	37.92	35.42	29.6	36.31	31.48	13.35
Molar Mass (g/mol)	102.03	114.04	114.04	99.72	108.6	108.43	118.73	66.05
Latent Heat @−15°C (kJ/kg)	209.5	195.6	180.3	214.7	203.64	194.1	186.3	329.9
Refrigerant Cost (USD)	$24.25	$74	$99.2	$25 **	$44.09	$55	$50 **	$15.51
Reference for Refrigerant Cost	[36, 37]	[38]	[39]		[40]	[41]		[42]

*A1 (Non-flammable) A2L (Mildly flammable) A2/A3 (Flammable)

** The refrigerant prices here are estimated based on the blended proportion.

The coefficient of performance (COP) of the overall DMS-VCRS is obtained from Eqs. (4).

$$COP = \frac{\dot{Q}_{evap}}{\dot{W}_{Comp,Total} + \dot{W}_{Fan}} = \frac{\dot{Q}_{evap}}{\dot{W}_{Comp1} + \dot{W}_{Comp2} + \dot{W}_{Fan}} \quad (4)$$

The total exergy $\dot{Ex}$ of a system or component can be divided into two components: physical exergy $\dot{E}_{PH}$, and chemical exergy $\dot{E}_{CH}$, which is not considered here. [43]

$$\dot{Ex} = \dot{Ex}_{PH} + \dot{Ex}_{CH} = \dot{M}_{fs}(\dot{e}x_{PH} + \dot{e}x_{CH}) \quad (5)$$

The physical exergy component $\dot{e}_{PH}$ arises from the pressure differential between the fluid stream and the ambient environment [34].

$$e_{PH} = (h - h_0) - T_0(s - s_0) \quad (6)$$

Here h and s represent the specific enthalpy and entropy of a fluid stream under its actual operating conditions of temperature T and pressure p, while h_0 and s_0 represent the specific enthalpy and entropy of the same stream evaluated at reference environmental conditions T_o and P_o. For any component, the exergy balance is defined by the following Eqs. 7: [44]

$$Ex = \sum_j \left(1 - \frac{T_{ref}}{T_j}\right) Q_j - W_{CV} + \sum(Ex_{in} - Ex_{Out}) \quad (7)$$

Exergy destruction, which results from irreversibility's within the system, equals the difference between the total exergy entering and leaving the system. The general exergy balance equation is expressed as [45]:

$$\dot{E}x_{Dest} = \dot{E}x_{in} - \dot{E}x_{Out} \quad (8)$$

The Total Exergy Destruction ($\dot{E}_{Dest,Total}$), exergetic efficiency (η_{II}) and components relative irreversibility (RI_i) of DMS-VCRS are given by Eqs. (9, 10, & 11) below.

$$\dot{E}_{Dest,Total} = \dot{E}_{Dest,Evap} + \dot{E}_{Dest,Cond1} + \dot{E}_{Dest,Cond2} + \dot{E}_{Dest,Comp1} + \dot{E}_{Dest,Comp2} + \dot{E}_{Dest,Fan} + \dot{E}_{Dest,EV1} + \dot{E}_{Dest,EV2} \quad (9)$$

$$\eta_{II} = \frac{Ex_{Out}}{Ex_{In}} = 1 - \frac{Ex_{Dest,Total}}{Ex_{In}} \quad (10)$$

$$RI_i = \frac{\dot{E}x_{Dest,i}}{\dot{E}x_{Dest,Total}} \quad (11)$$

Where *I* represents the component of evaluation.

2.3.2 Economic analysis

The economic analysis begins by identifying all costs associated with the system. The total Cost rate for the DMS-VCRS represents the summation of these capital and maintenance costs, operational expenses, CO2 emission penalties and refrigerant leak cost.

Table 2

Parameters used for simulation

Component	Parameters with Values	
Compressor	Combined Electrical and Mechanical Efficiency: 0.9, Allowable Suction line Degree of superheating rise: 3°C Isentropic Efficiency $\eta_{is} = 0.85 - 0.046667(\frac{P_{dis}}{P_{suc}})$ [18]	
Condenser	Condenser Temperature:40°C (32°C – 52°C), Allowable sub-cooling: 2°C, Air flow calculation is based on Lower Terminal Temperature Difference: 2 °C, Tube's inner/outer diameter: 7.894/9.52 mm [89]*	
Evaporator	Evaporator Temperature: -5°C (6°C to -24°C), Allowable superheating: 5°C (Main Evaporator), Cabinet Average Temperature: -8.5°C, Air flow calculation is based on Lower Terminal Temperature Difference: 2 °C	
Sub-Cooler	DMS cycle (DMSC) Evaporating Temperature: 0°C (15°C to -11°C), Design Refrigerant charge Ratio: 0.15 (0.05 – 0.65), Degree of subcooling (22°C to 39.5°C), Degree of superheating: 1.5°C (1.5°C to 37.5°C)	
Condenser Cooling Fan and motor	Fan isentropic Efficiency: 0.865, Combined Electrical and Mechanical Efficiency: 0.9, Environment Temperature: 25 °C	
Economics Parameters [46, 87]	Maintenance factor, φ	1.06, 1.08**
	Interest rate, i	14%
	Plant life time, n	15 years
	Annual operational hours, N	5256 hours
	Electrical power cost, α_{elec}	0.06 USD/kWh
	Emission factor, μ_{CO2e}	0.968 kg/kWh
	Cost of CO_2 avoided, C_{CO2}	0.09 USD/kg of CO_2 emission
	Leakage rate/Recovery Factor	5% (2.5%**)/70% [88]

* System A2/A2L refrigerants (the choice is due to stricter safety standards)

** Same diameter dimension applied to evaporator and subcooler.

The system cost rate is the sum of equipment cost, installation and refrigerant cost. Therefore, the total plant cost rate for the DMS-VCRS is expressed as:

$$\dot{C}_{Total} = \bar{C}_K + \dot{C}_{Op} + \dot{C}_{env} + \dot{C}_{Refg,Leak} \quad (12a)$$

$\dot{C}_{Sys} = 1.07 * \sum_K \dot{C}_K + \dot{C}_{Installation} + \dot{C}_{Refg} + \dot{C}_{SysMod}$ (12b)

$\dot{C}_{Refg} = \dot{c}_{Refg} \times m_{Charge}$ (13)

$\dot{C}_{Refg,Leak} = \mathrm{L_{annual}} \times c_{Refg} \times m_{Charge}$ (14)

According to Sanaye and Malek Mohammadi [47], approximately 0.84% of the total investment cost is attributed to auxiliary components such as piping, expansion valves, and refrigerant.

Since the refrigerant and expansion valve costs are already included in the cost models, a 7% adjustment to the equipment capital cost is applied to account solely for system piping and system control unit (Eq. 12b), thereby accommodating the extended piping lengths adopted in the present modelling.

Eco-friendly refrigerants often operate at different pressures or exhibit mild flammability, making retrofitting of existing R134a systems impractical. Consequently, a system modification cost $\dot{C}_{SysMod}$ is introduced to capture the expenses associated with upgrading components to minimise leakage and integrating safety features for A2 and A2L refrigerants. This cost typically ranges between 10–40% of the conventional system cost [48–49]. In this present work, it is taken as 20%. Capital and maintenance cost rates for system components are estimated using cost correlations summarised in Table 5, derived from the works of Solanki et al. [46] and Mosaffa and Farshi [87].

$\bar{C}_K = [(1.07 * \sum_K \dot{C}_K + \dot{C}_{SysMod}) \times \varphi + \dot{C}_{Installation} + \dot{C}_{Refg}] \times \mathrm{CRF}$ (15)

Where the maintenance factor of the plant is denoted by φ (Table 2).

Also, CRF, capital recovery factor, is determined using Eqs. 16: [46, 50]

$CRF = \frac{i(i+1)^n}{(i+1)^n - 1}$ (16)

The total capital investment and maintenance cost rate for the entire system is determined by summing the capital investment and maintenance costs of all individual components, expressed as:

$\sum_K \dot{C}_K = \dot{C}_{Comp1} + \dot{C}_{Cond1} + \dot{C}_{Evap} + \dot{C}_{EV1} + \dot{C}_{Comp2} + \dot{C}_{Cond2} + \dot{C}_{SubC} + \dot{C}_{EV2} + \dot{C}_{Fan1} + \dot{C}_{Fan2}$ (17)

The operational cost of the system encompasses the electricity consumption cost and is given by:

$\dot{C}_{Op} = N \times \dot{W}_{Total} \times \alpha_{\mathrm{elec}}$ (18)

The heat transfer surface area of the heat exchanger (A) for economic analysis is given by [46]:

$A = \frac{\dot{Q}}{U_0 LMTD}$ (19)

To estimate the heat transfer areas of the condenser, evaporator, and sub cooler for equipment cost evaluation, the overall heat transfer coefficient was determined using the governing equations and parameters presented in Table 4.

2.3.3 *Environmental analysis*

The penalty cost rate for greenhouse gas (GHG) emissions from the DMS-VCRS is calculated using the relationship established by Wang et al. [52] as:

$\dot{C}_{env} = m_{CO_2e} \times C_{CO_2}$ (20)

The annual greenhouse gas emission from the system (m_{CO2e}) is determined as [52]:

$m_{CO_2e} = \mu_{CO_2e} \times E_{Annual}$ (21)

The input parameter values assumed for the comprehensive system analysis are presented in Table 2.

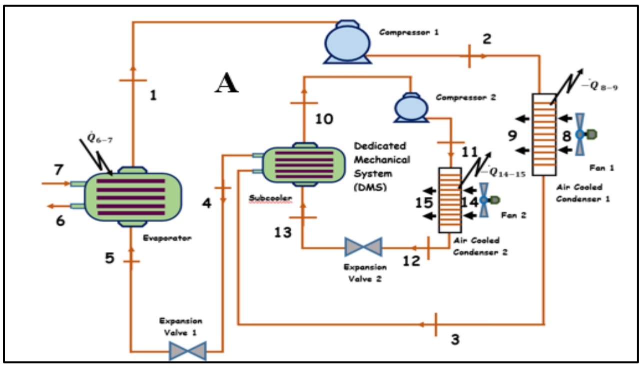

Fig. 2a. A diagram of a DMS-VCRS.

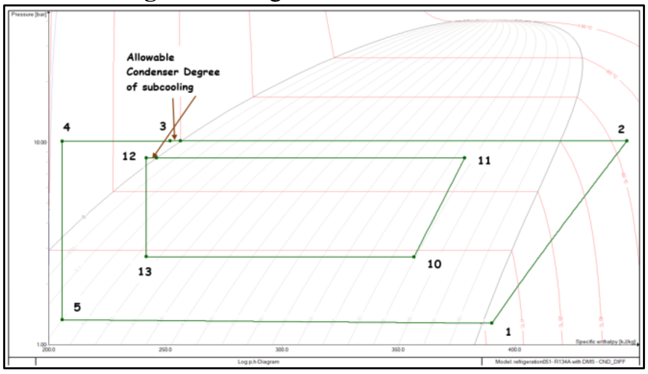

Fig. 2b. A P-h diagram of a DMS-VCRS.

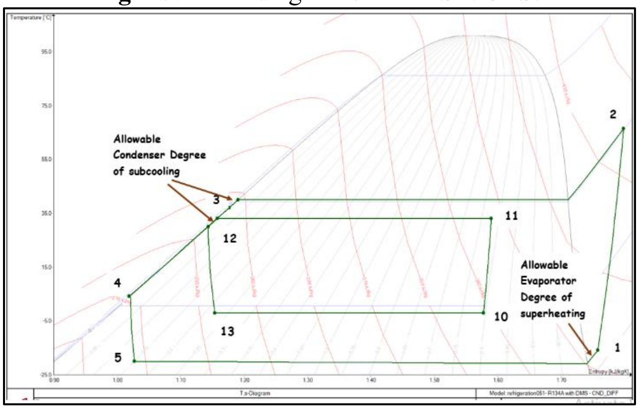

Fig. 2c. A T-s diagram of a DMS-VCRS.

2.4 *Total Equivalent Warming Impact (TEWI) Analysis*

The environmental evaluation was performed using the TEWI, which accounts for both direct and indirect greenhouse gas emissions [53, 54]:

$TEWI = TEWI_{direct} + TEWI_{indirect}$ (22)

Direct emissions result from refrigerant leakage and end-of-life loss [53], [55]:

$$TEWI_{direct} = \left(GWP \cdot L_{annual} \cdot n + GWP \cdot M_{total} \cdot (1 - \alpha_{recovery})\right) \quad (23)$$

where:

$$L_{annual} = M_{total} \cdot \frac{\text{Leakage Rate}}{100} \quad (24)$$

Indirect emissions result from energy consumption [53, 54]:

$$TEWI_{indirect} = E_{annual} \cdot n \cdot \beta \quad (25)$$

where:

$$E_{annual} = \frac{Q_{cooling} \cdot t_{operation}}{COP} \quad (26)$$

Total TEWI is given as:

$$TEWI = GWP \cdot M_{total}\left[\frac{\text{LR}}{100} \cdot n + (1 - \alpha_{recovery})\right] + \frac{Q_{cooling} \cdot t_{operation} \cdot n \cdot \beta}{COP} \quad (27)$$

2.5 Refrigerant Charge Estimation

The total refrigerant charge in the system is computed as the sum of refrigerant mass in all components:

The total refrigerant charge in the system is calculated as [56, 57]:

Table 3

Energy and Exergy relations of the Main and subcooling sub-system of the DMS-VCRS.

Components	Energy Relations	Exergy Relations	
		Exergy Destruction	Exergy Efficiency
Evaporator	$\dot{Q}_{Evap} = \dot{Q}_{6-7} = \dot{m}_{R1}(h_1 - h_5) = U_{Evap}A_{Evap}LMTD_{Evap}$	$\dot{E}x_{Dest,Evap} = Ex_5 - Ex_1 + \dot{Q}_{6-7}\left(1 - \frac{T_0}{T_{Evap}}\right)$	$\eta_{Ex,Evap} = 1 - \frac{\dot{E}x_{Dest,Evap}}{Ex_5 - Ex_1}$
Condenser 1	$\dot{Q}_{Evap} = \dot{Q}_{8-9} = \dot{m}_{R1}(h_2 - h_3) = U_{Cond1}A_{Cond1}LMTD_{Cond1}$	$\dot{E}x_{Dest,Cond1} = Ex_2 - Ex_3 - \dot{Q}_{8-9}\left(1 - \frac{T_0}{T_{Cond,Ave1}}\right)$	$\eta_{Ex,Cond1} = 1 - \frac{\dot{E}x_{Dest,Cond1}}{Ex_2 - Ex_3}$
Condenser 2	$\dot{Q}_{Evap} = \dot{Q}_{14-15} = \dot{m}_{R2}(h_{11} - h_{12}) = U_{Cond2}A_{Cond2}LMTD_{Cond2}$	$\dot{E}x_{Dest,Cond2} = Ex_{11} - Ex_{12} - \dot{Q}_{14-15}\left(1 - \frac{T_0}{T_{Cond,Ave2}}\right)$	$\eta_{Ex,Cond2} = 1 - \frac{\dot{E}x_{Dest,Cond2}}{Ex_{11} - Ex_{12}}$
Sub cooler	$\dot{m}_{R1}(h_4 - h_3) = \dot{m}_{R2}(h_{10} - h_{13})$ $\epsilon = \frac{T_{Cold,out} - T_{Cold,in}}{T_{Hot,in} - T_{Cold,in}} = \frac{T_{10} - T_{13}}{T_3 - T_{13}}$	$\dot{E}x_{DestSubC} = Ex_{13} - Ex_{10} + (Ex_3 - Ex_4)$	$\eta_{Ex,SubC} = 1 - \frac{\dot{E}x_{DestSubC}}{Ex_{13} + Ex_3}$
Compressor 1	$\dot{W}_{Comp1} = \frac{\dot{m}_{R1}(h_2 - h_1)}{\eta_{Isen} \times \eta_{Mech-Elect}}$	$\dot{E}x_{Dest,Comp1} = Ex_2 - Ex_1 + \dot{W}_{Comp1}$	$\eta_{Ex,Comp1} = 1 - \frac{\dot{E}x_{Dest,Comp1}}{Ex_2 - Ex_1}$
Compressor 2	$\dot{W}_{Comp2} = \frac{\dot{m}_{R2}(h_{11} - h_{10})}{\eta_{Isen} \times \eta_{Mech-Elect}}$	$\dot{E}x_{Dest,Comp2} = Ex_{11} - Ex_{10} + \dot{W}_{Comp2}$	$\eta_{Ex,Comp2} = 1 - \frac{\dot{E}x_{Dest,Comp2}}{Ex_{11} - Ex_{10}}$
Condenser Fan	$\dot{W}_{Fan} = \dot{W}_{Fan1} + \dot{W}_{Fan2} = \frac{\dot{m}_{Air1}(h_9 - h_8)}{\eta_{Isen,Fan} \times \eta_{Mech-Elect}} + \frac{\dot{m}_{Air2}(h_{15} - h_{14})}{\eta_{Isen,Fan} \times \eta_{Mech-Elect}}$	$\dot{E}x_{Dest,Fan} = (Ex_9 - Ex_8 + Ex_{15} - Ex_{14}) - \dot{W}_{Fan}$	$\eta_{Ex,fan} = 1 - \frac{\dot{E}x_{Dest,Comp1}}{(Ex_9 - Ex_8 + Ex_{15} - Ex_{14})}$
Expansion Valve 1	$h_4 = h_5$	$\dot{E}x_{Dest,EV1} = Ex_4 - Ex_5$	$\eta_{Ex,Ev1} = 1 - \frac{\dot{E}x_{Dest,Ev1}}{Ex_4}$
Expansion Valve 2	$h_{12} = h_{13}$	$\dot{E}x_{Dest,EV2} = Ex_{12} - Ex_{13}$	$\eta_{Ex,Ev2} = 1 - \frac{\dot{E}x_{Dest,Ev2}}{Ex_{12}}$

$$M_{total} = M_{comp} + M_{cond} + M_{evap} + M_{subcooler} + M_{pipes} \quad (28)$$

The vapour fluid charge in the compressor (Mcomp) has been neglected [57].

For two-phase heat exchangers (evaporator, condenser sections), the refrigerant charge is [57, 58]:

$$M_{2\phi} = \int_0^L \rho_{tp} \cdot A_c \, dz \quad (29)$$

where the two-phase density is:

$$\rho_{tp} = \rho_L(1 - y) + \rho_V \cdot y \quad (30)$$

The mean void fraction over the heat exchanger length is calculated as [58]:

$$\overline{y} = \frac{1}{L}\int_0^L y \, dz = \frac{1}{x_o - x_i}\int_{x_i}^{x_o} y \, dx \quad (31)$$

where y is the local void fraction using Zivi correlation [58], [59]:

$$y = \frac{1}{1 - \frac{1-x}{x}S} = \frac{x}{S + (S-1)x} \quad (32)$$

The slip ratio parameter is defined as [58]:

$$S = \left(\frac{\rho_V}{\rho_L}\right)^{\frac{2}{3}} \quad (33)$$

where:

x_i = vapour quality at inlet, x_o = vapour quality at outlet, ρ_V = vapour density (kg/m³), ρ_L = liquid density (kg/m³)

Substituting the local void fraction in equ. (36) into the mean void fraction equation:

$$\overline{y} = \frac{1}{x_o - x_i}\int_{x_i}^{x_o} \frac{x}{S + (S-1)x} \, dx \quad (34)$$

This integral solution, analytically with further simplification, is given as:

$$\overline{y} = 1 + \frac{S}{(S-1)(x_o - x_i)} \ln\left(\frac{S + (S-1)x_o}{S + (S-1)x_i}\right) \quad (35)$$

Using the mean void fraction and two-phase mass charge [57]:

$$\overline{\rho}_{tp} = \rho_L(1 - \overline{y}) + \rho_V \cdot \overline{y} \quad (36)$$

$$M_{2\phi} = \overline{\rho}_{tp} \cdot V_{internal} \quad (37)$$

For pipeline sections, an average constant void fraction approach is adopted, and the pipe length was scaled as 15% of the heat exchanger length. The void fraction is assumed constant throughout the pipe length based on inlet conditions:

The refrigerant mass in pipelines with two-phase flow is:

$$M_{Pipe} = V_{Pipe} \times \left(\alpha_{Pipe} \times \rho_v + \left(1 - \alpha_{Pipe}\right) \times \rho_L\right) \quad (38)$$

For single-phase pipeline sections:

$$M_{Sp} = V_{Int} \times \rho \quad (39)$$

where ρ is the refrigerant density (kg/m³), and V_{Int} is the internal volume (m³) of the component or pipe.

2.9 Safety Analysis for Flammable Refrigerants

A comprehensive safety assessment was conducted for A2 and A2L refrigerants in compliance with IEC 60335-2-89:2019 [60]. The revised standard, following a five-year review, increased allowable charge limits in self-contained commercial systems to 500 g for A3 refrigerants (R290, R600a) and 1.2 kg for A2/A2L refrigerants (R152a, R440A, R1234yf, R1234ze(E), R32) to promote the adoption of low-GWP alternatives [61], [62].

Table 4

Heat transfer analysis for DMS-VCRS condensers and evaporator (applicable to subcooler).

Condenser and Evaporator Heat Transfer Analysis	Condenser	Evaporator
Desuperheating/Superheating Zone	$Q_{dsh} = \dot{m}_r \times \left(h_{sup} - h_g\right)$ $A_{dsh} = \frac{Q_{dsh}}{U_{dsh} \times LMTD_{dsh}}$ $U_{sh} = 150\ W/m^2.K$ [86]	$Q_{sup} = \dot{m}_r \times \left(h_{out} - h_g\right)$ $A_{sup} = \frac{Q_{sup}}{U_{sup} \times LMTD_{sup}}$ $U_{dsh} = 325\ W/m^2.K$ [86]
Condensing /Evaporating Zone	$Q_{cond} = \dot{m}_r \times h_{fg}$ $A_{cond} = \frac{Q_{cond}}{U_{cond} \times LMTD_{cond}}$ $U_{Cond} = 975\ W/m^2.K$ [86]	$Q_{evap} = \dot{m}_r \times h_{fg}$ $A_{evap} = \frac{Q_{evap}}{U_{evap} \times LMTD_{evap}}$ $U_{Evap} = 675\ W/m^2.K$ [86]
Subcooling Zone	$Q_{sub} = \dot{m}_r \times \left(h_f - h_{sub}\right)$ $A_{sub} = \frac{Q_{sub}}{U_{sub} \times LMTD_{sub}}$ $U_{Sub} = 240\ W/m^2.K$ [86]	
Total Area Calculation **Note:** LMTD for each zone	$A_{condenser} = A_{dsh} + A_{cond} + A_{sub}$ $LMTD = \frac{\Delta T_1 - \Delta T_2}{\ln\left(\frac{\Delta T_1}{\Delta T_2}\right)}$ Where: • ΔT_1 = Temperature difference at inlet • ΔT_2 = Temperature difference at outlet	$A_{evaporator} = A_{evap} + A_{sup}$

Flammability properties differ significantly among these fluids. R152a exhibits very low ignition energy (~0.004 mJ) with flammability limits of 3.9.–16.9 vol.% and an LFL of 0.092 kg/m³, whereas R440A shows 0.015 mJ and 0.097 kg/m³, respectively [63]–[66]. While R1234yf and R1234ze(E) require higher ignition energies (25–50 mJ and 7–20 mJ) and exhibit higher LFLs (0.289 and 0.303 kg/m³), indicating lower ignition susceptibility [65], [67].

IEC 60335-2-89 mandates risk-control provisions including leak prevention, charge limitation, and active ventilation. Systems with less than 1200g of flammable refrigerant will employ hydrocarbon-sensitive leak detectors (activating at 50% LEL). It may also employ continuous ventilation (≥0.4 m/s), hermetically sealed compressors, and explosion-proof (IP65-rated) electrical components within 3 m of potential leak sources [70]–[74]. All installations must continue to adhere to ISO 5149, EN 378, and ASHRAE 15 standards [75]–[78]. Recent research confirms that, with appropriate mitigation measures, A2/A2L refrigerants can be safely used in commercial refrigeration without sacrificing performance, according to recent studies [68, 69].

Table 5

Cost functions of the system components [46, 51, 87]

Component	Capital Cost Function
Compressor (1 & 2)	$C_{Comp,1\,\&\,2} = \left(\frac{573 \times \dot{m}_R}{0.8996 - \eta_{Isen}}\right)\left(\frac{P_{Cond}}{P_{Evap}}\right) In \left(\frac{P_{Cond}}{P_{Evap}}\right)$
Evaporator	$C_{Evap} = 516.621 \times A_{Evap} + 268.45$
Condenser (1 & 2)	$C_{Cond\ 1\&\,2} = 516.621 \times A_{Cond} + 268.45$
Evapansion Valve (1 & 2)	$C_{Ev\ 1\&2} = 114.5 \times \dot{m}_{1,2}$
Subcooler	$C_{SubC} = 516.621 \times A_{SubC} + 268.45$
Condenser Fan	$C_{Fan\ 1\&2} = 155 \times (\dot{V} + 1.43)$
Installation Cost	$C_{Installation} = 150.2 \times \dot{Q}_{Evap}$

Table 6

Performance comparison of current model with Solanki et al [18] and Agarwal et al [16] examining the influence of condenser temperature on refrigerant R134a (Tevap = − 10 °C, Tcond = 40 °C)

Condenser Temp.	COP [16, 18]	COP (Present Model)	Exergy Eff. [18]	Exergy Eff. [16]	Exergy Eff. (Present Model)	Error in % COP [16, 18]	Error in % Exergy Eff. Compared to [18]	Error in % Exergy Eff. Compared to [16]
30	4.5199	4.5946	49.9870	50.7179	51.4034	1.6261	2.755	1.333
35	3.8914	3.9495	43.5129	43.8205	44.1857	1.4696	1.523	0.826
40	3.3933	3.4264	38.3460	37.9616	38.3341	0.9683	-0.031	0.972
45	2.9674	2.9918	34.0256	33.2563	33.4720	0.8157	-1.654	0.644
50	2.6140	2.6231	30.2820	29.2436	29.3462	0.3461	-3.189	0.349
Mean Error						1.045	-0.119	0.825

Table 7

Statistical validation metrics for the present model compared to literature data

Parameter	Reference	RMSE	MAPE (%)	R^2	Standard Deviation
COP*	[16] & [18]	0.0334	1.382	0.9996	0.0318
Exergy Efficiency	[16]	0.8617	1.848	0.9988	0.6431
Exergy Efficiency	[18]	1.2738	2.755	0.9972	0.6126

**Literature [16] and [18] report identical COP values, hence a single comparison for COP*

3. Results And Discussion

This study presents energy, exergy, economic and environmental analyses of DMS-VCRS with a condenser cooling fan designed for cold storage applications. Environmentally friendly refrigerants assessed as R134a alternatives are: R1234ze(E), R1234yf, R440A, R450A, R513A, R515A, and R152A. The parametric study investigates how condenser and evaporator temperatures, superheating and subcooling degrees, and refrigerant mass flow ratio affect system performance using 4Es analysis.

3.1 Model Validation

Model validation was conducted through comparison with theoretical studies by Solanki et al. [18] and Agarwal et al. [16] to confirm the accuracy and dependability of the DMS-VCRS model developed in STEAG Ebsilon. The simulated results show strong agreement with literature data, with respect to the coefficient of performance (COP) and exergy efficiency (η_II)across the condenser temperature range of 30–50 °C. For COP validation, the comparison shows excellent agreement (RMSE = 0.0334, MAPE = 1.382%, R^2 = 0.9996). For exergy efficiency, it showed closer alignment with Agarwal et al. [16] (MAPE = 1.848%) than with Solanki et al. [18] (MAPE = 2.755%), with both maintaining high correlations (R^2 > 0.997). These results prove the model's predictive reliability, with MAPE < 1.5% for COP and < 3% for η_II, validating its applicability for R134a-based system design and optimisation (see Fig. 3, Tables 6 and 7).

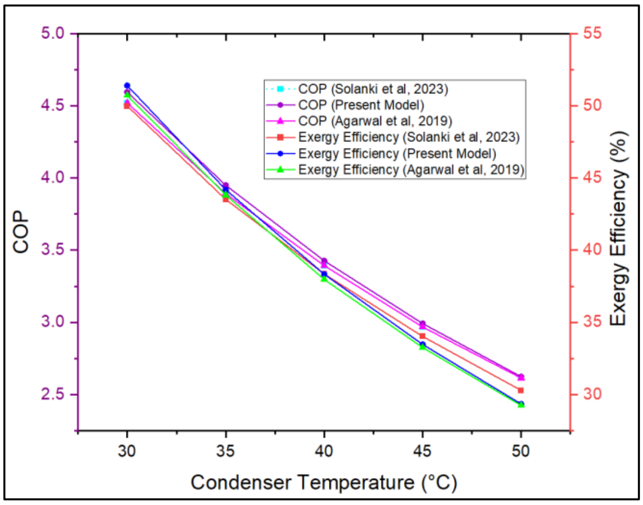

Fig. 3. A performance comparison of the current model's results against N. Solanki et al. [18] and Agarwal et al. [16]. It demonstrates how condenser temperature affects R134a performance at an evaporator temperature of -10°C.

3.2 Relative Capacity Indices

Figure 4 presents information on the several evaluated relative capacity indices of seven low-GWP refrigerants compared to R134a. It shows the available results of the assessment of performance differences for the metrics evaluated.

Among the low-GWP refrigerants, R152a and R440A displayed the greatest improvements in COP and η_II exceeding 2.9%. They offered lower mass flow rates and compressor discharge pressure, leading to smaller compressor sizing and lower compressor work. This explains their superior COP performance over R134a substitutes. The results validate previous studies that R152a is a preferred low-GWP alternative to R134A with superior performance [80].

R513A, R515A, R450A, R1234yf, and R1234ze(E) exhibit slight COP decrease relative to R134a. These refrigerants exhibit either high compressor pressure ratios or increased mass flow rates, resulting in higher compressor work, as reported by Sánchez et al. [9]. R513A and R450A showed a reasonable drop in compatibility with R134A, displaying similar discharge temperatures, pressures, and cooling capacities. This observation aligns with Makhnatch et al. [54], who identified R513A as a practical retrofit option requiring minimal system modifications.

In summary, R152A and R440A offer the best thermodynamic performance among the evaluated refrigerants for new designs, while R513A provides a well-balanced drop-in option with minimal changes required for existing VCRS.

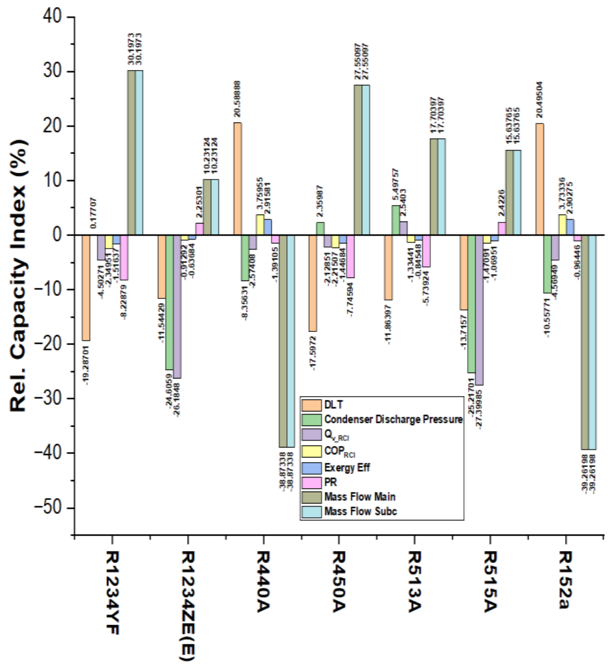

Fig. 4. Relative capacity index (%) of discharge line temperature (DLT), condenser discharge pressure, volumetric cooling capacity (VCC), COPRCI, exergy efficiency (ηII_RCI), pressure ratio (PRComp), refrigerant charge flow in main cycle (MRefg,MS) and subcooling system (MRefg,SS) of alternative refrigerants compared to R134a in a DMS-VCRS.

3.3 Relative Irreversibility And Exergy Efficiency Evaluation

As shown in Figure 5(a), Compressor 1 accounted for the largest share of system irreversibility, exceeding 34% for all refrigerants. R134a and R1234ze(E) had the highest values. In contrast, R152a and R513A showed lower irreversibility in Compressor 1, indicating better thermodynamic performance.

The evaporator and Condenser 1 contributed moderately (14–20%) to total irreversibility, while the subcooler, valves, and fan showed minor impacts (<10%), consistent with reported trends in ancillary component behaviour [81], [82].

Exergy efficiency trends (Figure 5(b)) reflected the inverse of these findings. The subcooler and expansion valves maintained high exergy efficiencies (over 90%) for all refrigerants, indicating minimal entropy generation. Condensers 1 and 2 had the lowest efficiencies, especially for R440A (28.9% and 32.3%) and R152A (29.5% and 33.1%). Overall, R152A and R440A achieved the highest exergy performance with lower irreversibility, confirming their suitability as effective, low-impact substitutes for R134a [12].

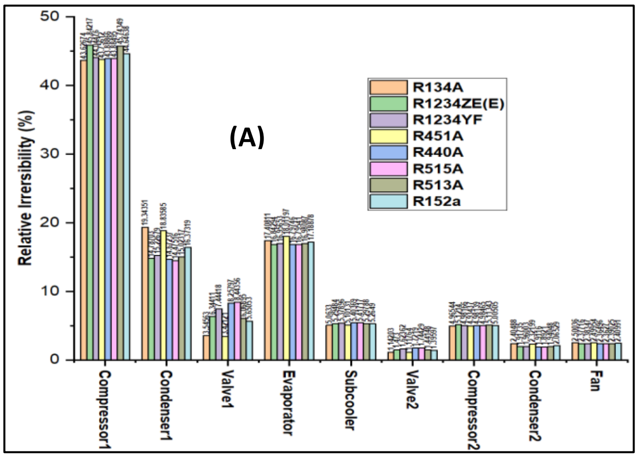

Fig. 5a. The Relative Irreversibility (%) of various components in DMS-VCRS for different refrigerants under consideration.

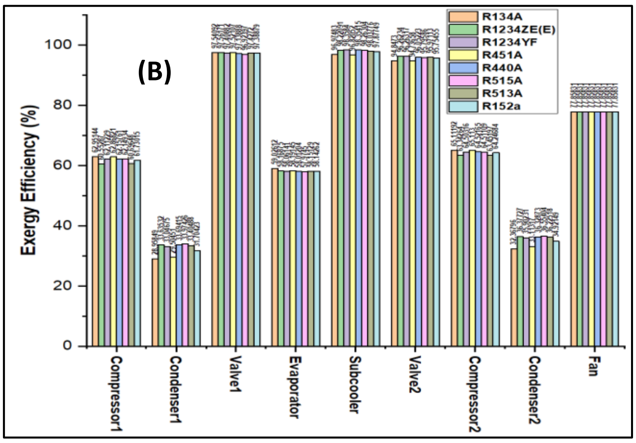

Fig. 5b. Exergy efficiency (%) of various components in DMS-VCRS for different refrigerants under consideration.

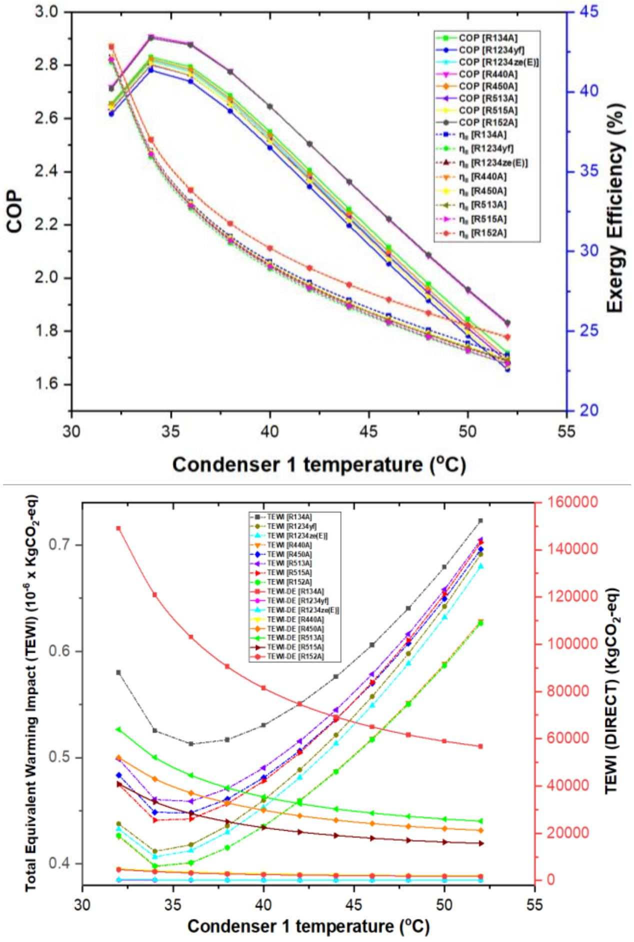

Fig. 6. Effect of Condenser 1 temperature on system performance:

(a) coefficient of performance (COP) and exergy efficiency (%).

(b) total equivalent warming impact (Total TEWI) and Direct TEWI.

3.4 Effect of Condenser Temperatures on System Performance

Condenser temperatures were varied from 32°C to 52°C across eight refrigerants. This variation revealed distinct performance characteristics for the two condensers. Fig. 6(a) shows that condenser 1 exhibits a pronounced parabolic COP trend. It rises from 2.6–2.65 at 32 °C, reaching a maximum of 2.9 (for R152A, R440A) and 2.78 (for R1234yf) at 34–35 °c. It then declines sharply to 1.7–1.8 at 52 °C, representing approximately 40% performance degradation. Exergy efficiency shows a consistent decline from 42% at 32°C to 23% at 52°C (Fig. 6(a)).

Figures 7(a–b) show that condenser 2 exhibits a linear COP decrease from 2.76–2.90 to 2.65–2.72. Exergy efficiency also shows a steady decline from 35.2% to 32.0%, indicating more stable operational behaviour. Economic evaluation reveals a clearly different cost behaviour between the two condensers. According to Figs. 6(c) and (d), the annual total cost rate (ATCR) of Condenser 1 takes the form of a U-shape that exhibits minimum values in the range 6.3 to 6.85 × 10³ USD yr-1 at around 34 to 36 °C. Subsequently, the ATCR will increase to the range of 8.6 to 9.7 × 10^3 USD yr^{-1} at about 52 °C. TCR-SYS exhibits parabolic behaviour, reaching a maximum of around 14 × 10^3 USD (for R1234yf) and 11.7 × 10^3 USD (for R134A) at about 40 °C. The ATCR of Condenser 2 (Figs. 7(c–d)) also increasing linearly from 6.3–6.9 × 10^3 USD yr^{-1} to 6.6–7.2 × 10^3 USD yr^{-1}, and its TCR-SYS is stable at 12.0–12.2 × 10^3 USD (R134A) and 14.2–14.3 × 10^3 USD (R1234yf).

The environmental assessment (Figs. 6(b) and 7(e–f)) indicates condenser 1 exhibits U-shaped total TEWI variation with minimum values of 0.40–0.53 × 10^6 kg CO_2-eq at 34–35 °C. It increases to 0.63–0.73 × 10^6 kg CO_2-eq at 52 °C, representing a 27% reduction from optimal temperature. Direct TEWI decreases steadily with temperature, with its average value less than 15% of TEWI Total, indicating indirect emissions dominate the overall impact. Condenser 2 shows a parabolic direct TEWI with minima at 38–42 °C, and total TEWI increases slightly by approximately 4%.

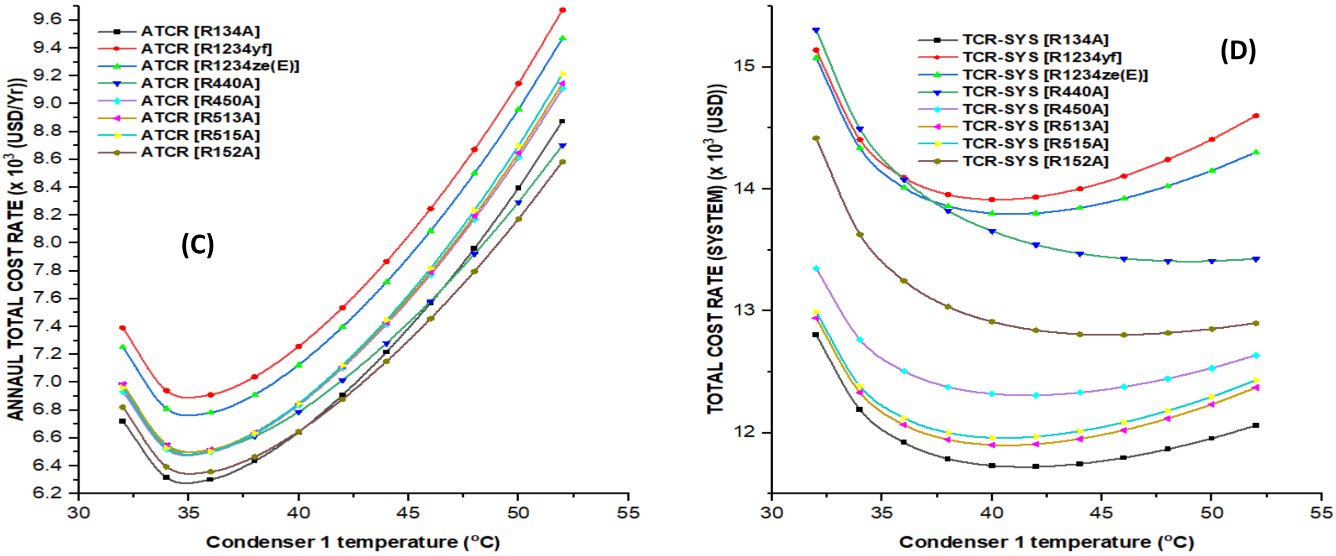

Fig. 6b. Effect of Condenser 1 temperature on system performance:

(c) Annual total cost rate (ATCR),

(d) Total system cost (TCR-SYS).

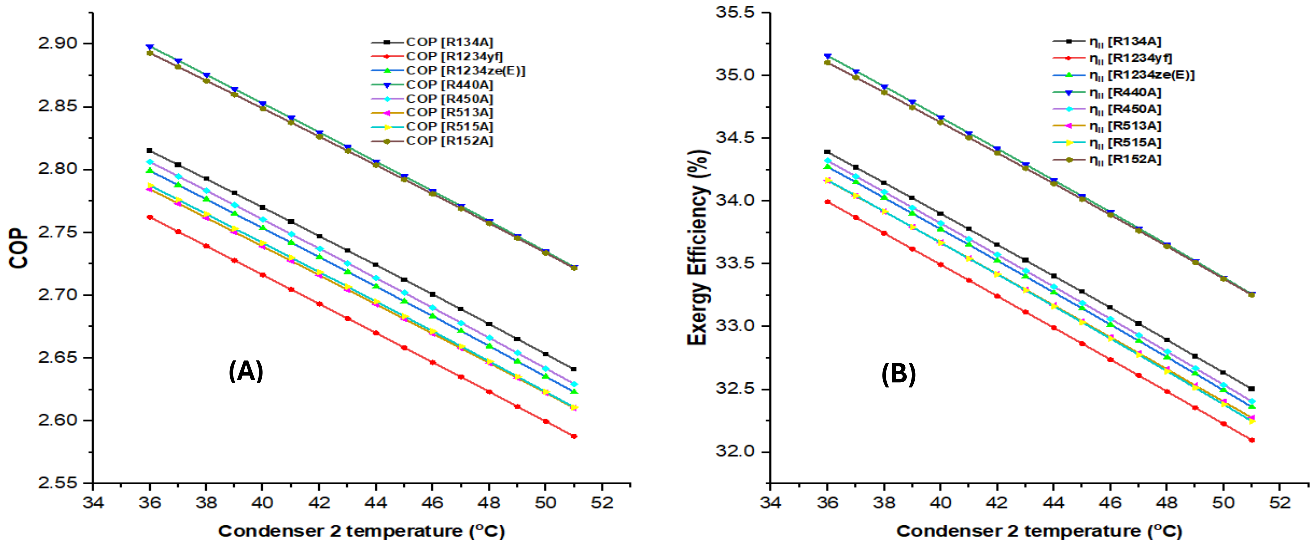

Fig. 7. Effect of Condenser 2 temperature on system performance:

(a) COP,

(b) Exergy efficiency (%).

The comparative assessment of direct TEWI between two condensers indicates that condenser 1 has an optimal temperature range of 34 to 40 °C, while condenser 2 provides show optimal temperature that is refrigerant dependent.

In summary, R152A and R440A exhibit superior performance compared to R134A among the evaluated refrigerant alternatives, achieving a 2–7% increase in COP, a 1.4–5% increase in η_II, -3.3–+1.5% ATCR increase, 7-13% TCR-SYS increase while 5-12% TCR-SYS decrease (compare to R1234yf), and a 13–26% reduction in Total Equivalent Warming Impact (TEWI) compare to R134a. These findings aligned with Aprea et al. [8]. Finally, optimal condenser sizing, effective temperature management, and careful refrigerant selection in system design will improve both system performance and environmental sustainability.

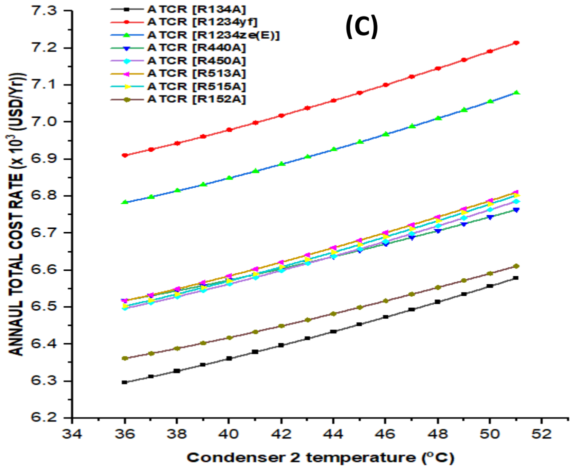

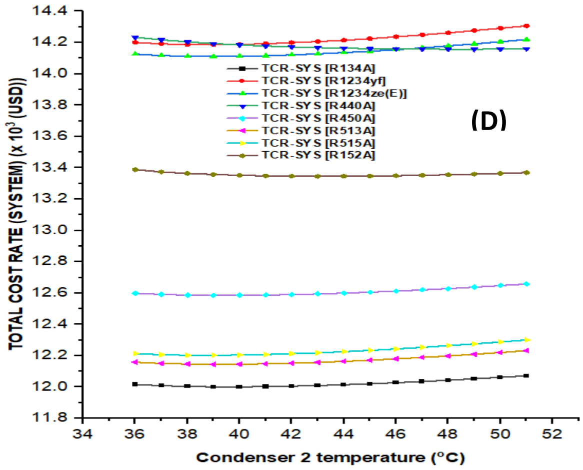

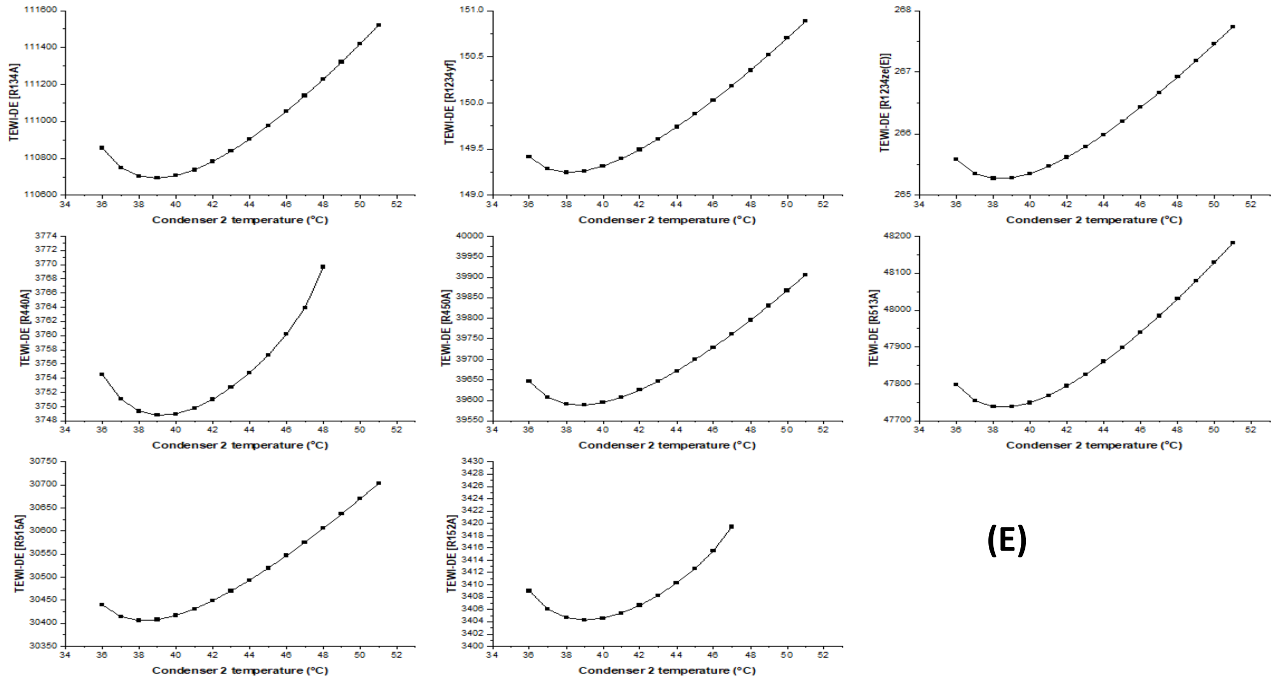

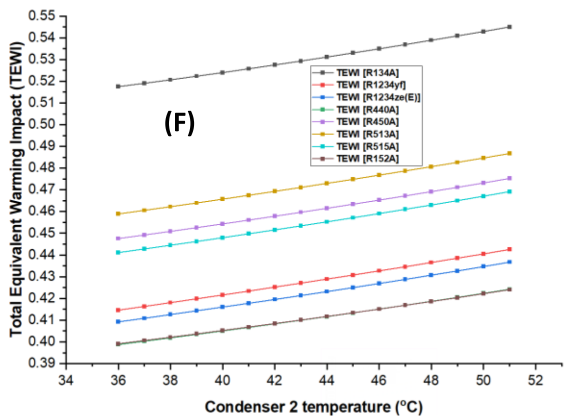

Fig. 7. Effect of Condenser 2 temperature on system performance:

(c) ATCR,

(d) TCR-SYS,

(e) Direct TEWI,

(f) Total TEWI.

3.5 Influence of Evaporator Temperatures on System Performance

The evaporator temperatures range for the main and subcooling cycles are examined from -24 °C to 6 °C and -11 °C to 15 °C. For the main evaporator, Fig. 8(a) shows that COP gradually rises from 1.0 at -24 °C to 3.9–4.0 at 6 °C for R152A and R440A, and 1.0–3.8 for R1234yf. This represents a fourfold improvement, suggesting reduced compressor workload and improved thermal integration. Exergy efficiency shows non-linear changes, rising from 21–22% at -24 °C to peak values of 28.9–30.2% near -4 °C, before slightly declining to 26.7–27.8% at 6 °C. This indicates optimal operation and minimised irreversibilities at approximately −4 °C [83].

Economic evaluation (Figs. 8(c–d)) shows ATCR decreasing from 14.4–17.7 × 10^3 USD yr^{-1} to 5.5–6.0 × 10^3 USD yr^{-1}, while total system cost declines from 13.7–16.8 × 10^3 USD to 11–12.9 × 10^3 USD. Reduced energy demand and smaller equipment sizing result in a lower cost of 4–6% R152A than R134.

Environmental assessment (Figs. 8(b&e)) indicates exponential TEWI decline from 1.06–1.23 × 10^6 kg CO_2-eq to 0.29–0.37 × 10^6 kg CO_2-eq—nearly 90% reduction. Direct TEWI for R134A decreases from 96,000 to 77,000 kg CO_2-eq, and for R1234yf from 134 to 104 kg CO_2-eq, confirming the environmental benefits of higher evaporator temperatures.

For the subcooling cycle evaporating temperature, similar trends are observed (Figs. 9(a–b)). COP increases nearly linearly from 2.35–2.50 to 2.64–2.80 as the temperature rises from −11°C to 15°C. Exergy efficiency improves from 28.7% to 31.7%, consistent with Qin et al. [84] findings concerning elevated evaporator conditions.

Economic behaviour (Fig. 9(c)) follows mild parabolic trends: ATCR decreases from 6.9–7.6 × 10^3 USD yr^{-1} to minimum values of 6.49–6.63 × 10^3 USD yr^{-1} around 13 °C, while total system cost shows minima of 14.2–14.5 × 10^3 USD between 1–11°C, indicating thermodynamic and cost advantages coincide within this range.

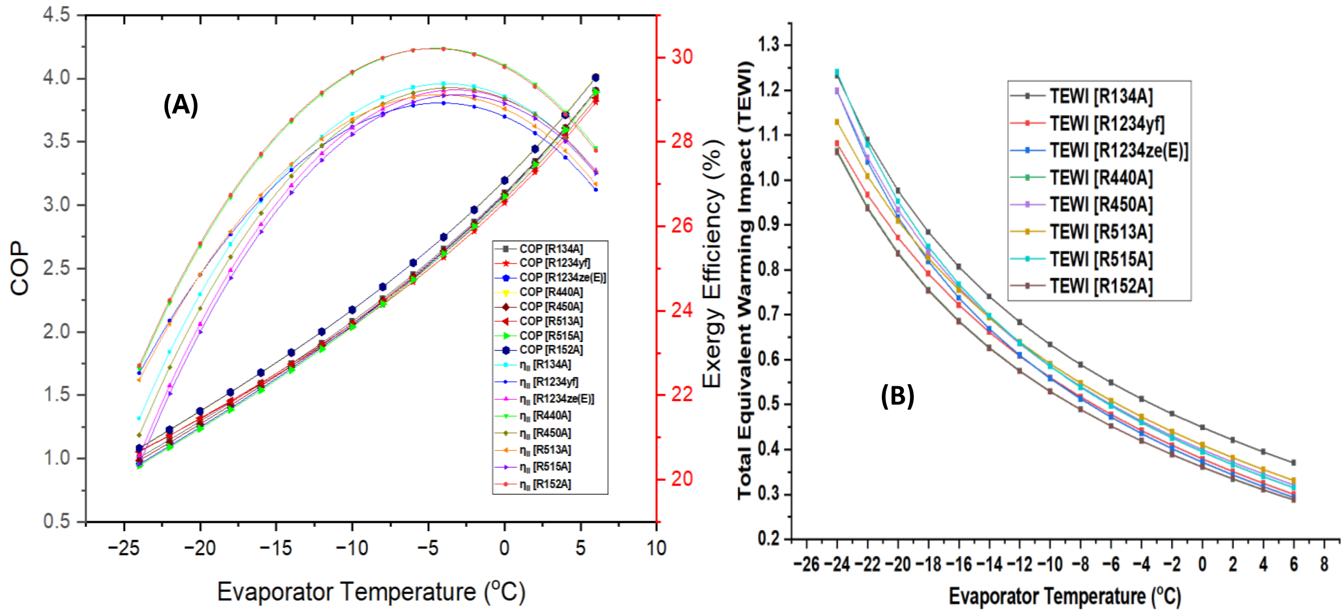

Fig. 8. Effect of main evaporator temperature on system performance:

(a) COP and exergy efficiency (%)

(b) Total TEWI

Environmental performance (Figs. 9(d–e)) exhibits parabolic direct TEWI variation with minima around 4–11°C. R134A records 81,757–81,306 kg CO_2-eq, while R1234yf shows 110–111 kg CO_2-eq. Total TEWI demonstrates a linear decrease from 0.46–0.48 × 10^6 kg CO_2-eq to 0.41–0.43 × 10^6 kg CO_2-eq. Among the refrigerants evaluated, R152A achieves the lowest total environmental impact, while R1234yf yields the highest environmental impact.

In conclusion, improvements in the thermodynamic and economic performance are observed with rising evaporator temperatures, with ηII reaching a maximum near −4 °C. To sum up, R152A & R440A exhibited a better performance than R134A: 2.5–7% rise in COP, 1.8–6% increase in ηII, -5.5–+2.2% increase in ATCR, 5-13% increase in TCR-SYS, but 9-15% (compared to R1234yf) and 14–22% decrease in TEWI. Based on findings, optimising the evaporator temperature is key to achieving a balance between energy efficiency, economic cost and environmental sustainability.

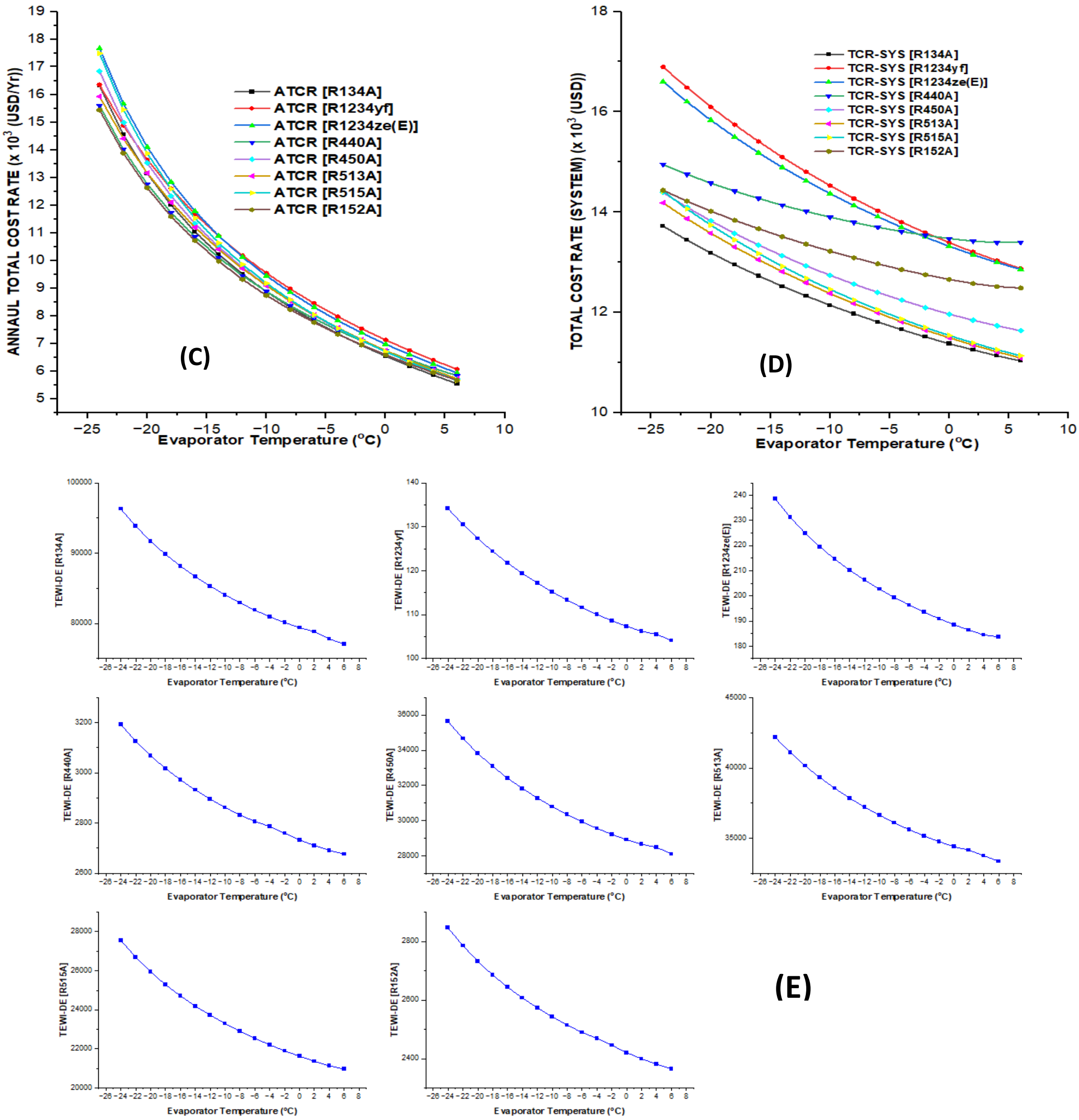

Fig. 8. Effect of main evaporator temperature on system performance:

(c) ATCR;

(d) TCR-SYS;

(e) Direct TEWI.

3.6 Effect of Circuit Refrigerant Mass Flow Ratio

The refrigerant mass flow ratio was evaluated across the range of 0.05–0.65. The excessive mass flow ratio of refrigerant causes instability in operations and elevated pinch point temperature in heat exchangers.

Figs. 10(a–b) shows a distinct and steady decline of COP and exergy efficiency with increasing refrigerant mass flow ratio. They decrease from 1.59–1.69 and 25.5–27.2% at 0.05 to 1.43–1.50 and 23.6–24.5% at 0.6—representing 9–14% degradation.

The COP and exergy efficiency performance of R152A and R440A remains the best, followed by R513A, R134A and R1234yf. R1234ze(E), R450A and R515A exhibit the poorest performance due to higher irreversibility from greater friction and pressure losses.

Figs. 10(c–d) shows similar trends for economic performance. ATCR increases from 9.27–10.22 × 10^3 USD yr^{-1} to 10.3–10.8 × 10^3 USD yr^{-1} at 0.6, with R152A exhibiting lowest values and R515A, R1234yf, and R1234ze(E) highest, reflecting low-GWP market premiums. TCR-SYS rises from 12.7–15.4 × 10^3 USD to 14.1–16.5 × 10^3 USD at 0.6.

Fig. 10(e) shows a linear trend for environmental evaluation. Total TEWI increases from 0.68–0.80 × 10^6 kg CO_2-eq to 0.77–0.82 × 10^6 kg CO_2-eq at 0.6. R440A and R152A achieve the lowest values at 0.70–0.71 × 10^6 kg CO_2-eq when the ratio is 0.35, demonstrating excellent performance through enhanced efficiency and reduced indirect emissions.

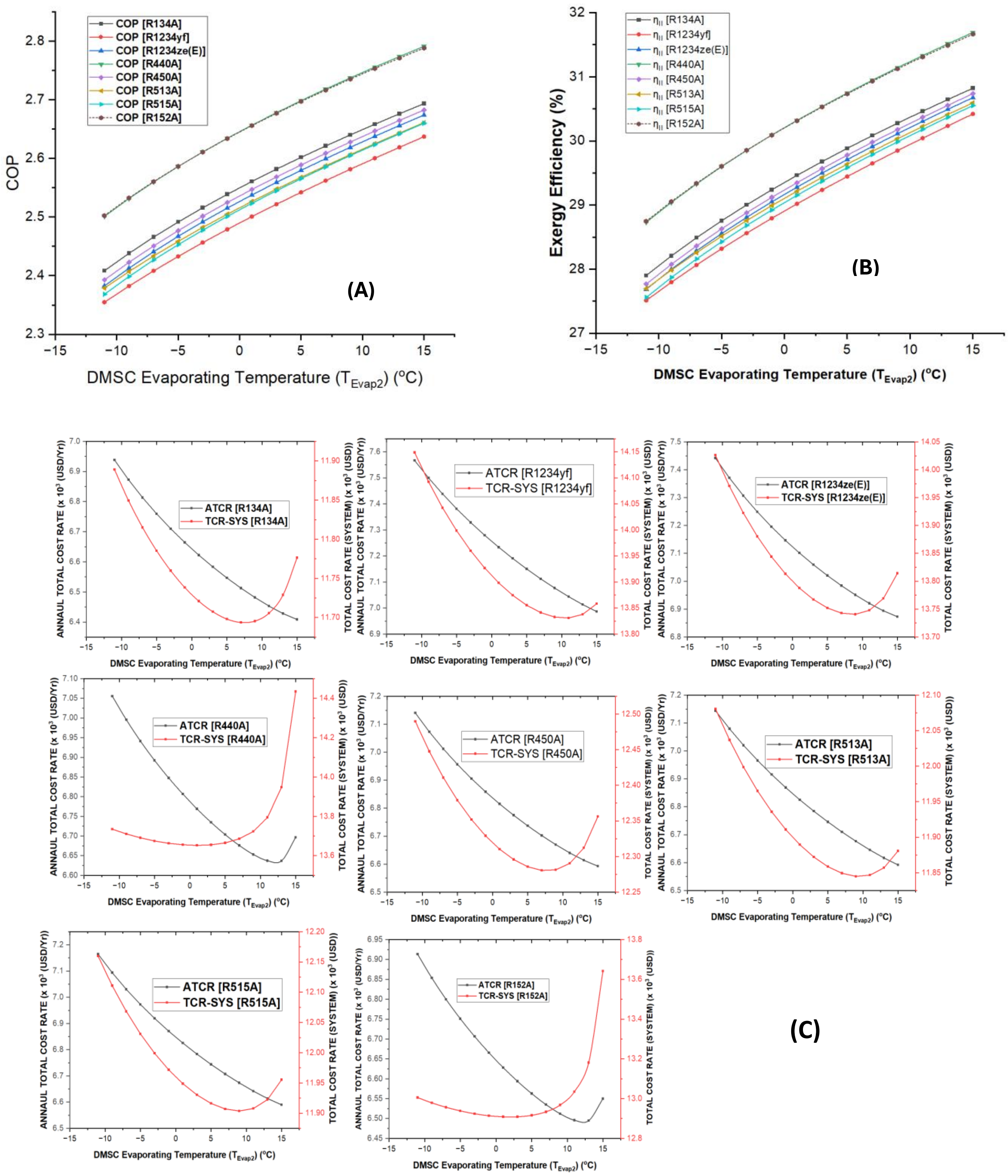

Fig. 9. Effect of secondary cycle evaporator temperature on system performance:

(a) Coefficient of performance (COP),

(b) Exergy efficiency,

(c) Annual total cost rate (ATCR) and Total system cost rate (TCR-SYS)

Direct TEWI (Figure 10(f)) exhibits strong refrigerant-specific behaviour: R134A shows substantially elevated values (715,000–763,000 kg CO_2-eq) owing to its high GWP, whereas low-GWP options contribute minimally. The declining trend indicates that direct emissions decrease as the mass flow ratio rises.

R152A emerges as the most promising R134a alternative, consistently outperform R134A, achieving 5% higher COP, 4.3% higher η_II, 3% lower ATCR, 6-7% higher TCR-SYS, but 9% lower to R1234yf, and 14–16% lower TEWI, which makes it a suitable candidate for sustainable medium-load refrigeration systems, provided safety measures address its mild flammability (A2 classification). R440A exhibits comparable performance with similar efficiency and favourable economic and environmental indices.

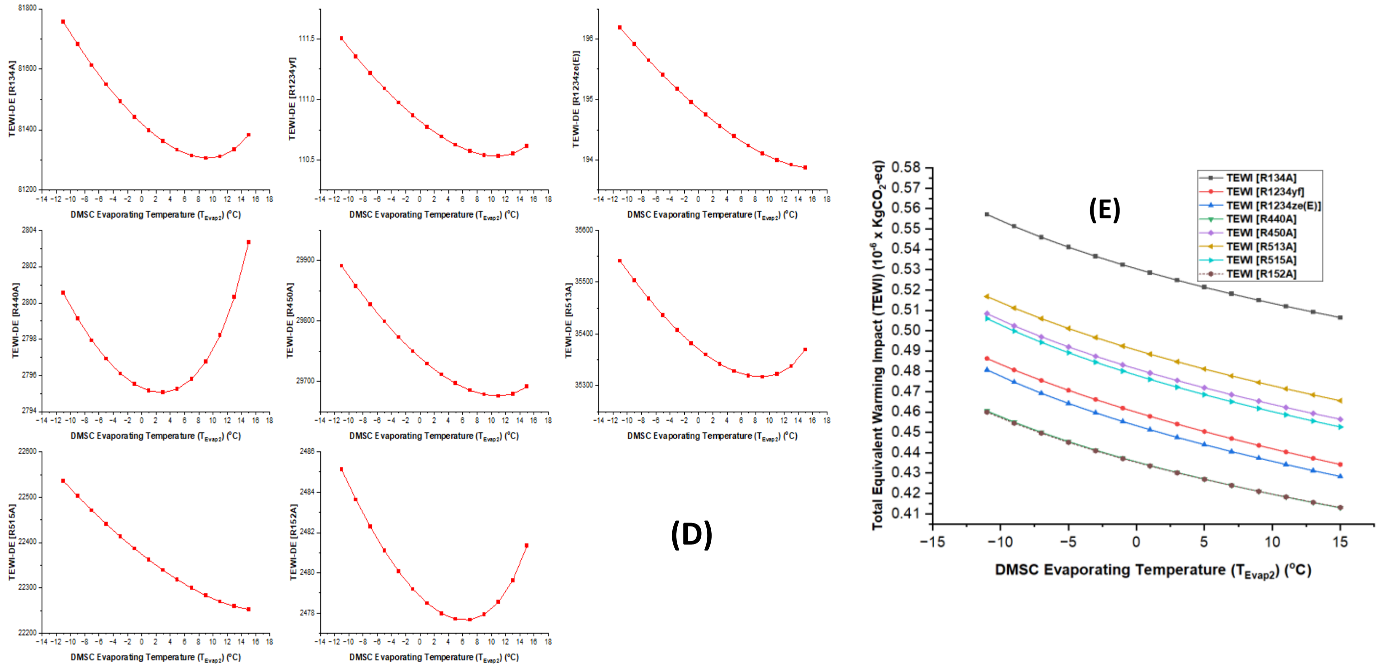

Fig. 9. Effect of DMSC evaporator temperature on system performance:

(d) Direct TEWI and,

(e) Total TEWI.

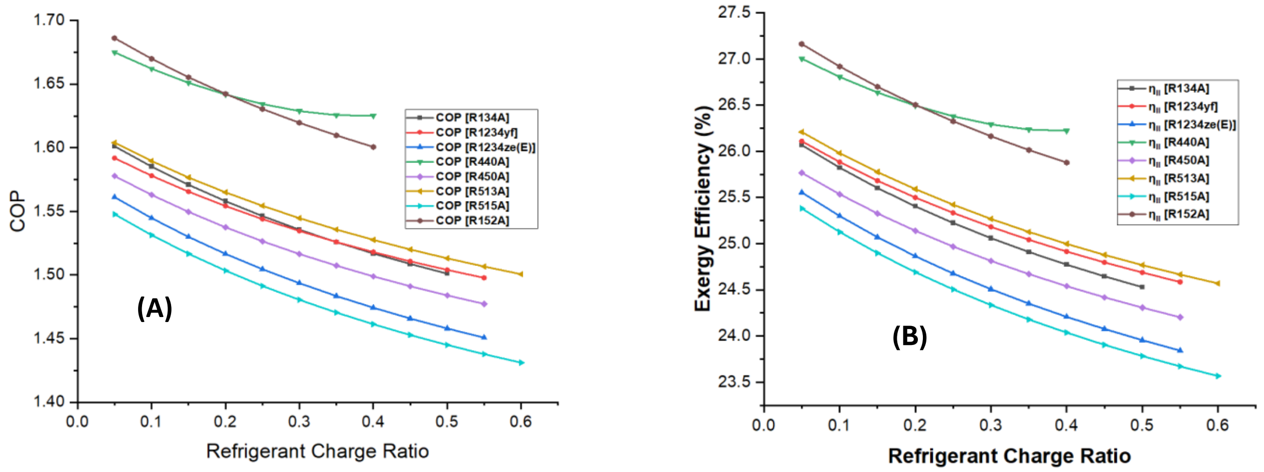

Fig. 10. Effect of refrigerant mass flow ratio on system performance:

(a) Coefficient of performance (COP);

(b) Exergy efficiency;

3.7 Effect Of Subcooler Degree Of Superheating And Subcooling

The degree of superheating and subcooling jointly influences the thermodynamic, economic, and environmental performance of the DMS-VCRS. The analysis covered superheating degree of 1.5–37.5 °C and subcooling of 22–39.5 °C, both limited by refrigerant and system reliability relating heat exchanger pinch point (Figures 11(a)–(e) & 12(a)–(h)). The subcooling range was selected to prevent wet vapour conditions at the subcooling cycle compressor inlet.

Increasing superheating and subcooling degrees provides a moderate but steady impact on system behaviour. For the superheating degree, the COP increases from 2.48–2.64 at 1.5 °C to 2.51–2.65 at 25.5 °C, and exergy efficiency improves from 28.8–30.2 % to 29.2–30.4%, indicating lower irreversibility. R440A and R152A achieve the highest COP (2.65 and 2.64 at 25.5 °C), followed by R134a, R450A, R1234ze(E), and R513A, while R1234yf and R515A perform slightly lower.

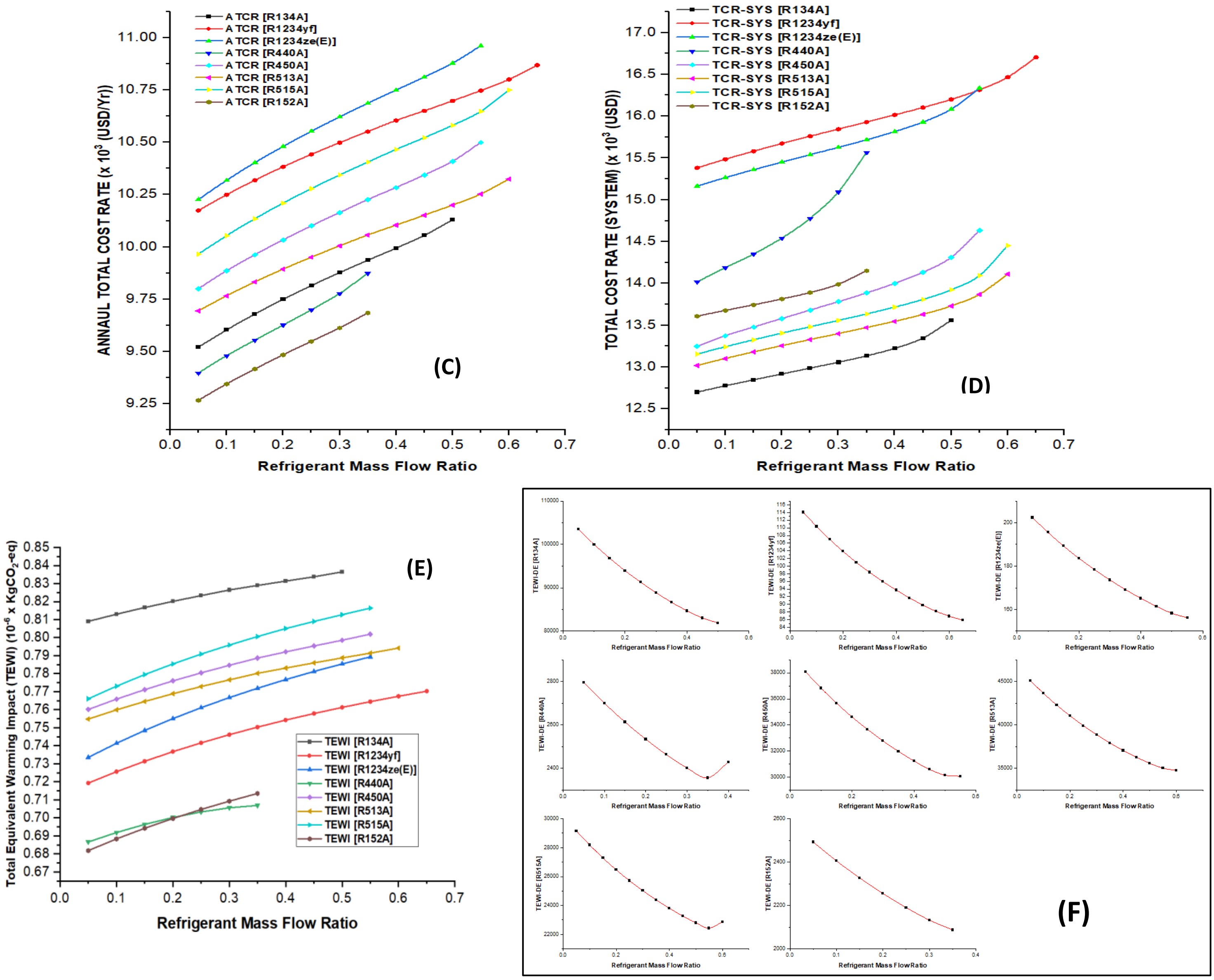

Fig. 10. Effect of refrigerant mass flow ratio on system performance:

(c) ATCR;

(d) TCR-SYS;

(e) Total TEWI;

(f) Direct TEWI.

Total TEWI decreases marginally from 0.43–0.53 × 10^6 kg CO_2-eq at 1.5 °C to 0.42–0.52 × 10^6 kg CO_2-eq at 25.5 °C, while direct TEWI remains nearly constant yet refrigerant-specific—highest for R134a (≈75,000 kg CO_2-eq) and lowest for R1234yf and R1234ze(E).

Economically, ATCR and TCR-SYS show non-linear trends. For R152A and R440A, an inflexion occurs near 22–23 °C, where compressor power begins to offset energy gains. R134a, R1234yf, R450A, R513A, and R515A show clear ATCR minima between 31–34 °C, where cost rates are lowest. For subcooling, both COP and η_II increase almost linearly across the stability-limited and wet-vapour-limited range (22–39.5 °C) due to a higher refrigerating effect. R152A and R440A also have superior thermodynamic performance with mild impact, as with other refrigerants. The ATCR and TCR-SYS vary non-linearly, with minima observed for R134A, R1234yf, R450A, R513A, and R515A at 27.3–32.5°C. Both total and direct TEWI remain relatively constant with slight reductions at higher subcooling levels, especially for R440A.

In summary, subcooling between 22–39.5 °C combined with moderate superheating (20–25 °C) yields modest improvements in system efficiency, exergetic performance, and environmental sustainability. R152A and R440A continue to represent the most favourable R134a alternatives from thermo-economic and environmental perspectives.

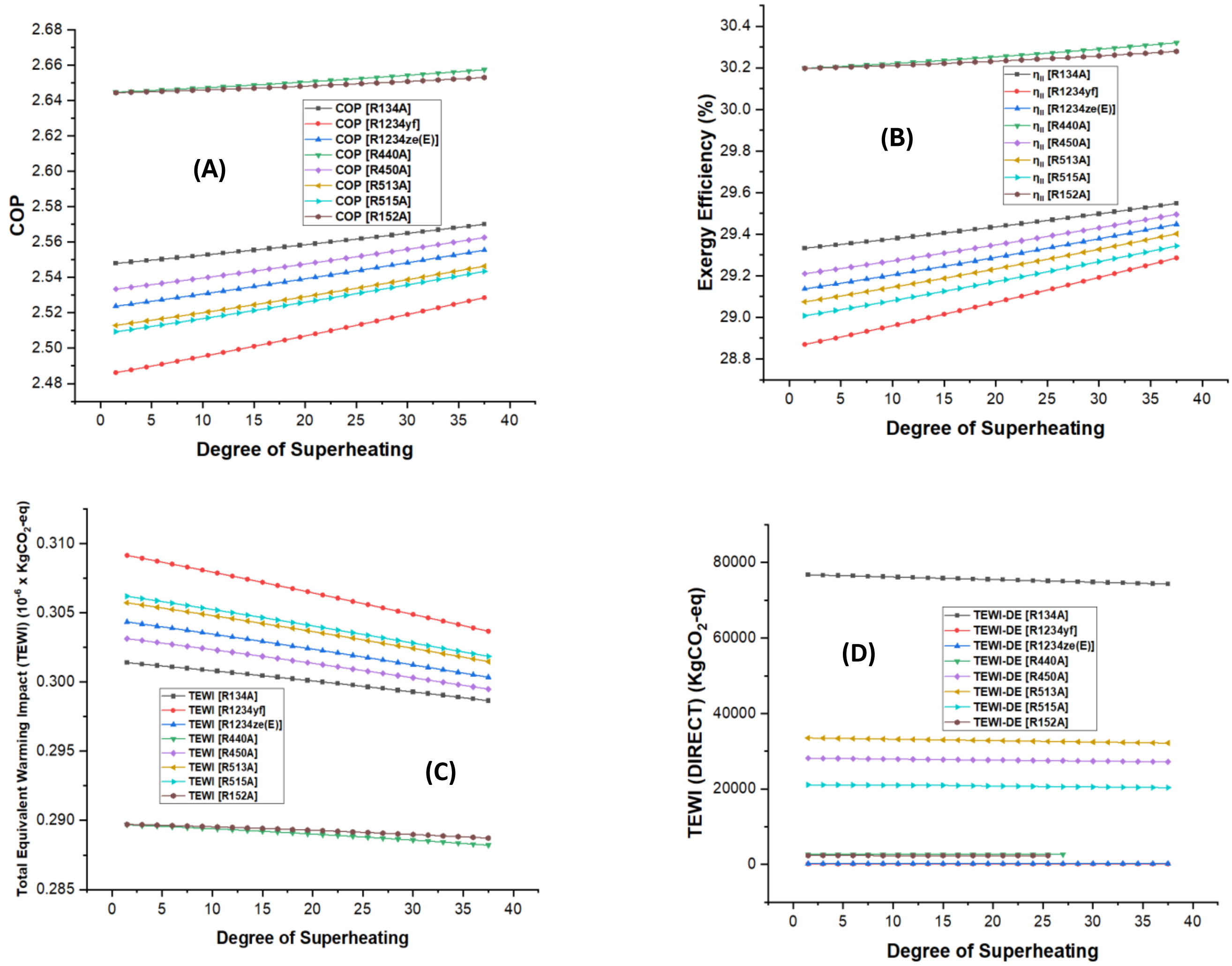

Fig. 11. Effect of degree of superheating on system performance:

(a) COP; (b) Exergy efficiency; (c) Total TEWI; (d) Direct TEWI; (e) ATCR and TCR-SYS.

4. Conclusion

A comprehensive parametric investigation of seven R134A replacements is conducted in this study, utilising a 4Es (Energy, Exergy, Economic, Environmental) analysis within a DMS-VCRS framework. It incorporates TEWI-based environmental analysis and safety-economic assessments for A2/A2L refrigerants. The STEAG Ebsilon Professional model developed in this study showed a strong correlation with the literature (RMSE = 0.0334, MAPE < 3%, R^2 > 0.997). Through our parametric analysis across varying condenser temperatures, evaporator temperatures, subcooling, and superheating degrees, we gained valuable insights into the reliable, safe working operation and optimal conditions for the system. The present study leads to the following deductions.

1. The thermodynamic performance shows that R152A and R440A exhibited superior performance, achieving 7% COP improvement and 6% exergy efficiency increase relative to R134a. This improvement is due to reduced compressor work and lower irreversibility losses. Across all evaluated refrigerants, more than 34% of the total system irreversibility was attributed to compressors, while subcoolers sustained the highest exergy efficiencies greater than 90%.
2. The economic analysis further indicates that the R152A and R440A system achieved an attractive economics compared to R134A. They record the lowest Annual Total Cost Rate (ATCR) (≈5% below R134a) and Total System Cost (TCR-SYS), which was roughly 9% higher than R134a (reflecting safety compliance modifications for A2/A2L refrigerants) but 12% lower than R1234yf. R513A and R450A proved to be moderate-priced solutions in retrofitting the R134A refrigeration system. Both showed average economic performance and have an A1 safety classification, which reduces the need for system modification while providing reasonable thermodynamic performance.

3. The environmental sustainability shows that TEWI analysis revealed that indirect emissions from electricity consumption dominated the environmental impact, exceeding 85% of total TEWI across all evaluated refrigerants. This emphasises why energy efficiency is critical for environmental performance than just refrigerant GWP. R152A and R440A achieved the best overall environmental performance, with TEWI values 13-26% lower than R134a. Although R1234yf and R1234ze(E) possess impressively low GWP values, their lower efficiency resulted in a higher total TEWI value, ranking them least among the refrigerants evaluated.
4. The range of operational conditions was carefully selected to avoid wet vapour formation at the suction end of the secondary cycle compressor of DMS-VCRS and ensure safe operation according to IEC 60335-2-89 for A2/A2L refrigerants. Finding reveals that subcooling and superheating degree variation showed a mild and consistent impact on 4Es performance.

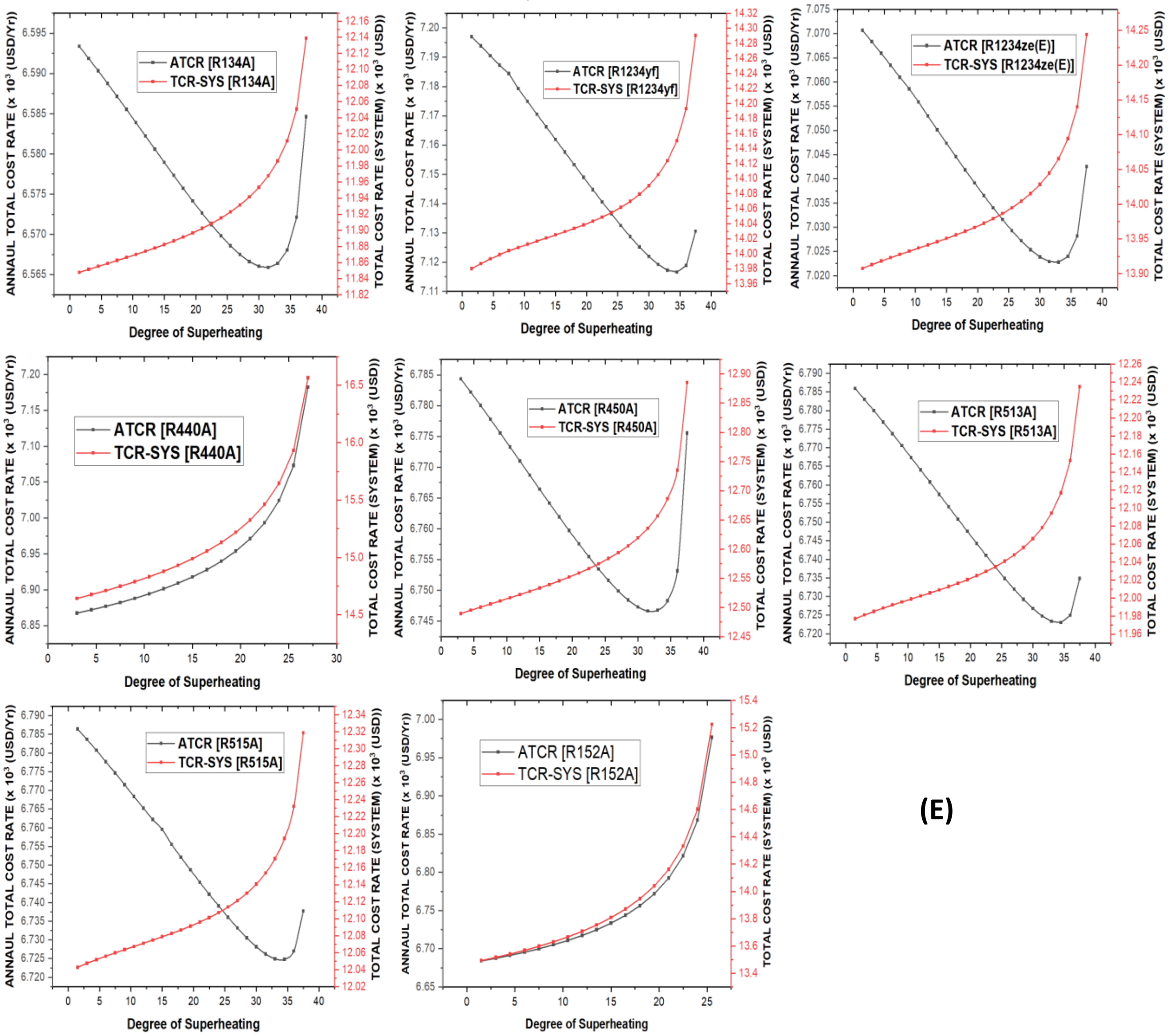

Fig. 11e. Effect of degree of superheating on system performance: ATCR [right] and TCR-SYS [left].

Secondly, optimal conditions were identified while varying the operational conditions: condenser 1 temperature of 34–37 °C, evaporator temperature of -4 °C, and superheating and subcooling degrees of 20–25 °C and 27.3–32.5 °C.

Based on our findings, R152A and R440A emerge as the most suitable substitutes for R134a, providing superior performance across all four criteria we evaluated. Their A2 flammability classification requires careful consideration; however, proper implementation of IEC 60335-2-89 guidelines—such as charge limitation (≤1.2 kg), leak detection, and adequate ventilation—facilitates their safe utilisation in commercial refrigeration applications. For situations where flammability concerns outweigh performance advantages, R513A represents the best non-flammable option, offering reasonable drop-in compatibility with minimal system modifications.

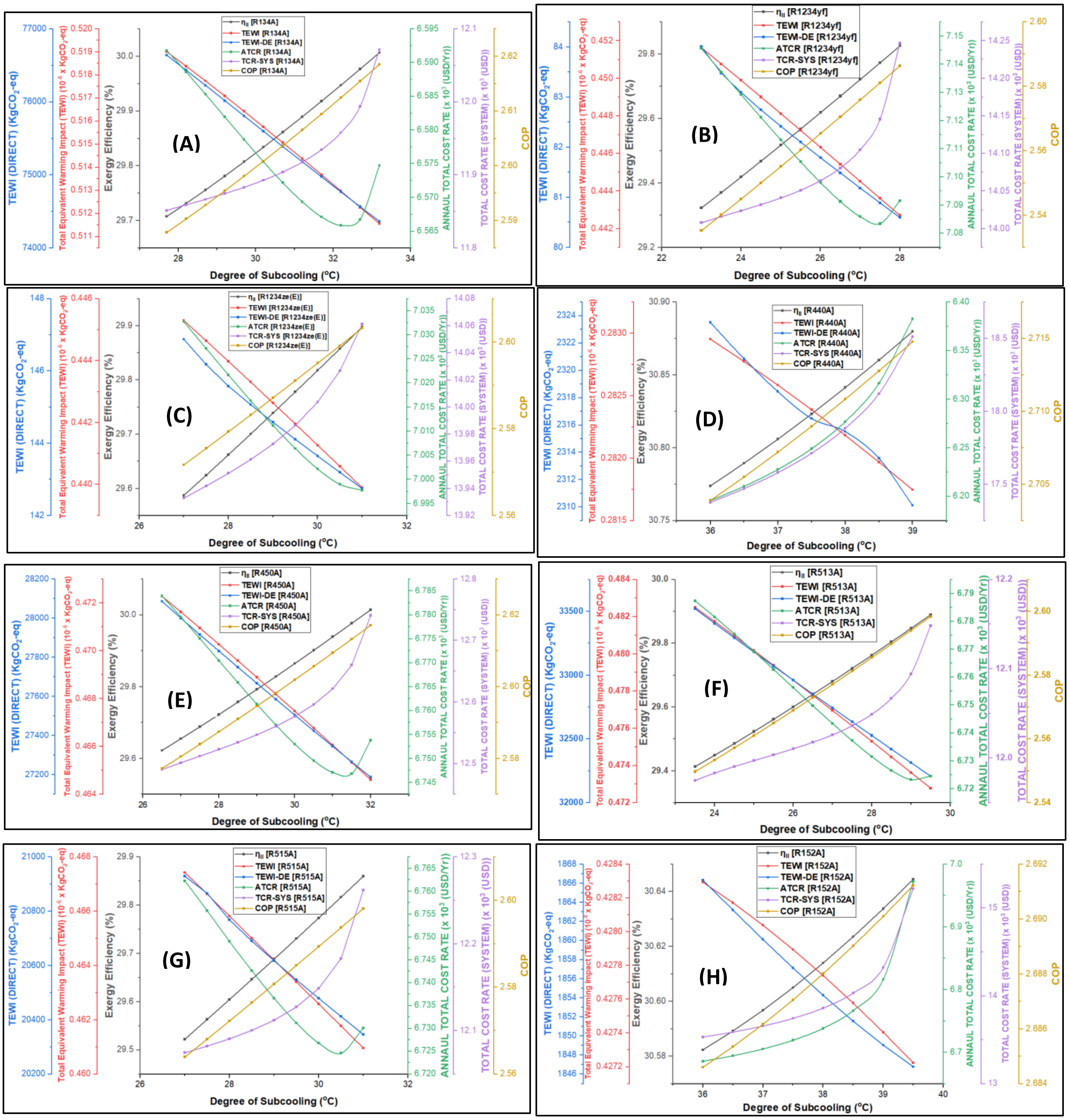

Fig. 12. Effect of degree of subcooling on system performance for all investigated refrigerants: COP, Exergy efficiency, ATCR, TCR-SYS, Total TEWI, TEWI (direct).

Nomenclature:

Acronyms:

DMS Dedicated Mechanical Subcooling

LMTD Log Mean Temperature Difference

RMFR Refrigerant mass flow ratio

VCRS Vapour Compression Refrigeration System

Symbols:

h Specific Enthalpy (kJ/kg)

P Pressure (kPa or Bar)

L Leakage rate

$\dot{m}$ Mass Flow Rate (kg/s)

$\dot{v}$ Specific Volume (m3/ kg)

P Pressure (kPa)

Q Heat Transfer Rate (kW)

T Temperature (°C or K)

W Work (kW)

S Entropy (kJ/kg·K)

Ex Exergy (kJ)

i Interest Rate (%)

n Operating Life (years)

N Annual Operating hours (Hrs)

A Heat exchanger surface area, m2

U Overall heat transfer coefficient (J/m2.K)

ΔTsc Degree of Subcooling (°C or K)

v specific volume of the refrigerant, m3/kg

PR Pressure ratio between high- and low-pressure side

Cco2 Penalty cost of CO2 emissions ($/tons of CO2 emission)

mco2 Annual emission of carbon dioxide (ton)

top Per-year operation period (h)

W Power input rate (kW)

Greek Symbols

ϵ Subcooler Effectiveness (dimensionless)

ȠII Exergy Efficiency (%)

Subscript:

i index for components in the DMS-VCRS

in inlet of the fluid to the device for consideration

out exit of the fluid from the device for consideration

Sat saturation

Ref Environment or reference property

0 Environment or reference property

Cond Condenser

comp Compressor

dsp Desuperheating

Evap Evaporator

refg Refrigerant

sh superheating

SubC Subcooler

sys System

tot Total

dis Discharge end of the compressor

suc Suction end of the compressor

fs Flowing stream.

5. References

[1] A. Tejani, H. Gajjar, V. Toshniwal, and R. Kandelwal, "The impact of low-GWP refrigerants on environmental sustainability: An examination of recent advances in refrigeration systems," ESP Journal of Engineering & Technology Advancements, vol. 2, no. 2, pp. 62–77, 2022.

[2] A. M. Ashour, S. A. Kadhim, H. M. Jaffar, O. A. A. M. Ibrahim, A. Mota-Babiloni, and A. Bouabidi, "Experimental investigation of the performance of vapor compression cycle in a water cooler system with low-GWP alternative refrigerants," Thermal Science and Engineering Progress, Art. no. 103611, 2025.

[3] A. Q. Abdelhamid, A. M. Abdel-Basier, M. K. Zakaria, and H. A. Abdelhalim, "Water and carbon footprint for different technologies of HVAC systems (vapor compression and gas absorption)," Egyptian Journal of Chemistry, vol. 68, no. 4, pp. 1–25, 2025.

[4] F. E. Sadni, I. Salhi, A. Hajjaji, Y. Boughaleb, and F. Belhora, "Energy and exergy analysis of basic organic Rankine cycle for waste heat recovery: A comparative study of organic fluids," in Proc. Int. Conf. Adv. Mater. for Photonics, Sensing and Energy Conversion—Energy Applications, Singapore: Springer, 2025, pp. 39–49.

[5] H. Zhang, S. Huang, L. Li, and S. Ouyang, "Prioritizing key factors in refrigerant substitution for GHG emission reduction: An integrated DEMATEL-ISM-MICMAC approach," Sustainability, vol. 17, no. 11, p. 5155, 2025.

[6] H. Iwasaki, N. Hoshiya, Y. Kishikawa, J. Escorihuela, and N. Shibata, "Repurposing HFC-125 to tetrafluoroethylene: A step toward a more sustainable fluoropolymer feedstock strategy," iScience, vol. 28, no. 6, 2025.

[7] S. I. Na, M. Kim, and M. S. Kim, "Performance simulation of CO2 transcritical cooling system with mechanical subcooling cycle for automobile air conditioning," J. Mech. Sci. Technol., vol. 36, no. 9, pp. 4797–4807, Sep. 2022.

[8] K. S. Hmood, V. Apostol, H. Pop, V. Badescu, and E. Pop, "Drop-in and retrofit refrigerants as replacement possibilities of R134a in domestic/commercial refrigeration and automobile air conditioner applications," J. Therm. Eng., vol. 7, no. 7, pp. 1815–1835, 2021, doi: 10.14744/jten.2021.0006.

[9] C. Aprea, A. Greco, and A. Maiorino, "An experimental investigation on the substitution of HFC134a with HFO1234YF in a domestic refrigerator," Appl. Therm. Eng., vol. 106, pp. 959–967, Aug. 2016, doi: 10.1016/j.applthermaleng.2016.06.098.

[10] D. Sánchez, A. Andreu-Nácher, D. Calleja-Anta, R. Llopis, and R. Cabello, "Energy impact evaluation of different low-GWP alternatives to replace R134a in a beverage cooler: Experimental analysis and optimization for the pure refrigerants R152a, R1234yf, R290, R1270, R600a and R744," Energy Convers. Manage., vol. 256, p. 115388, Apr. 2022, doi: 10.1016/j.enconman.2022.115388.

[11] Z. Hussain, N. You, and H. Cho, "Performance and energy evaluation of R450A, R1234yf, R513A, R516A, R152A, and R1234ze(E) as alternatives to R134A in an air conditioner," Appl. Therm. Eng., vol. 271, p. 126319, Jan. 2025.

[12] A. Mota-Babiloni, J. Navarro-Esbrí, Á. Barragán-Cervera, F. Molés, and B. Peris, "Analysis based on EU Regulation No 517/2014 of new HFC/HFO mixtures as alternatives of high GWP refrigerants in refrigeration and HVAC systems," Int. J. Refrig., vol. 52, pp. 21–31, 2015, doi: 10.1016/j.ijrefrig.2014.12.021.

[13] K. Nawaz, B. Shen, A. Elatar, V. D. Baxter, and O. Abdelaziz, "R1234yf and R1234ze(E) as low-GWP refrigerants for residential heat pump water heaters," Int. J. Refrig., 2017.

[14] B. Liu, Z. Yang, C. Zhang, Z. Lv, Y. Chen, and S. Chen, "Evaluation of a low-GWP and nonflammable blend as a new alternative for R134a in the heat pump system," Int. J. Refrig., vol. 143, no. 1, pp. 85–94, Nov. 2022, doi: 10.1016/j.ijrefrig.2022.06.029.

[15] B. O. Bolaji, "Theoretical assessment of new low global warming potential refrigerant mixtures as eco-friendly alternatives in domestic refrigeration systems," Scientific African, vol. 9, p. e00632, Nov. 2020, doi: 10.1016/j.sciaf.2020.e00632.

[16] G. Li, "Comprehensive investigation of transport refrigeration life cycle climate performance," Sustainable Energy Technologies and Assessments, vol. 21, pp. 33–49, 2017.

[17] S. Agarwal, A. Arora, and B. B. Arora, "Exergy analysis of dedicated mechanically subcooled vapour compression refrigeration cycle using HFC-R134a, HFO-R1234ze and R1234yf," in Advances in Energy and Built Environment. Singapore: Springer, 2020, pp. 23–33, doi: 10.1007/978-981-13-7557-6_3.

[18] N. A. Ansari, A. Arora, Samsher, and K. Manjunath, "The effect of eco-friendly refrigerants on performance of vapor compression refrigeration system with dedicated mechanical subcooling," in Advances in Energy and Built Environment. Singapore: Springer, 2020, vol. 36, doi: 10.1007/978-981-13-7557-6_4.

[19] N. Solanki, A. Arora, and R. K. Singh, "Performance enhancement and environmental analysis of vapor compression refrigeration system with dedicated mechanical subcooling," Int. J. Air-Cond. Ref., vol. 31, no. 26, 2023, doi: 10.1007/s44189-023-00042-8.

[20] T. S. Mogaji, A. Awolala, O. Z. Ayodeji, P. B. Mogaji, and D. E. Philip, "COP enhancement of vapour compression refrigeration system using dedicated mechanical subcooling cycle," Nigerian Journal of Technology (NIJOTECH), vol. 39, no. 3, pp. 776–784, Jul. 2020, doi: 10.4314/njt.v39i3.17.

[21] Q. Yang et al., "Thermodynamic analysis of an NH3/CO2 cascade refrigeration system with subcooling in the low-temperature circuit utilizing the expansion work," Int. J. Energy Res., vol. 2023, 5987368, 2023, doi: 10.1155/2023/5987368.

[22] Z. Zheng, Q. Yang, W. Zhang, Y. Zhao, G. Liu, and L. Li, "Thermodynamic analysis and comparison of mechanical subcooling transcritical CO2 refrigeration system with expander and throttling valve," Case Studies in Thermal Engineering, vol. 55, p. 105625, Dec. 2024, doi: 10.1016/j.csite.2024.105625.

[23] M. Deymi-Dashtebayaz, S. Ghorbani, H. Khabbazi, and M. Asadi, "4E analysis and multi-objective optimization of an ejector-expansion cascade refrigeration system for building cold storage using low GWP refrigerants," J. Build. Eng., vol. 98, p. 111470, Mar. 2024, doi: 10.1016/j.jobe.2024.111470.

[24] K. Kizilboga, A. Z. Sahin, B. Zafer, and I. H. Sahin, "Evaluation of low GWP refrigerants as alternatives for R134a in a vapor compression refrigeration cycle under varying operating [conditions]," Iraqi Academic Scientific Journals, Jan. 2025.

[25] L. V. S. Martins, C. H. M. Braga, J. J. G. Pabon, L. Machado, and W. M. Duarte, "Assessment of total equivalent warming impact (TEWI) of alternative refrigerants for

retrofit of R22 in single split air conditioning system," J. Build. Eng., vol. 88, Art. no. 109085, 2024, doi: 10.1016/j.jobe.2024.109085.

[26] R. Llopis, D. Calleja-Anta, A. Maiorino, L. Nebot-Andrés, D. Sánchez, and R. Cabello, "TEWI analysis of a stand-alone refrigeration system using low-GWP fluids with leakage ratio consideration," Int. J. Refrig., vol. 118, pp. 279–289, 2020, doi: 10.1016/j.ijrefrig.2020.05.028.

[27] I. Kayes, R. E. Ratul, A. Abid, F. B. Majmader, Y. Khan, and M. M. Ehsan, "Multi-objective optimization and 4E (energy, exergy, economy, environmental impact) analysis of a triple cascade refrigeration system," Heliyon, vol. 10, no. 11, e31655, May 2024.

[28] Y. Wang, H. Wang, and Z. Ma, "Techno-economic analysis of low-GWP refrigerants in refrigeration systems," Energy Reports, vol. 5, pp. 207–215, 2019.

[29] Z. Yang, X. Wang, and Y. Li, "Thermodynamic and economic analysis of a dedicated mechanical subcooling system for refrigeration applications," Energy, vol. 225, p. 120271, Jun. 2021, doi: 10.1016/j.energy.2021.120271.

[30] P. Makhnatch, A. Mota-Babiloni, A. López-Belchí, and R. Khodabandeh, "R450A and R513A as lower GWP mixtures for high ambient temperature countries: Experimental comparison with R134a," Energy, vol. 166, pp. 223–235, Jan. 2019, doi: 10.1016/j.energy.2018.10.065.

[31] STEAG Energy Services GmbH, EBSILON® Professional Software Documentation, 2024. [Online]. Available: https://www.ebsilon.com/en/downloads

[32] E. W. Lemmon, I. H. Bell, M. L. Huber, and M. O. McLinden, NIST Standard Reference Database 23: REFPROP, Version 10.0, 2023.

[33] ASHRAE, ANSI/ASHRAE Standard 34-2022: Designation and Safety Classification of Refrigerants. Atlanta, GA: ASHRAE, 2022.

[34] M. Direk, M. S. Mert, E. Soylu, and F. Yuksel, "Experimental investigation of an automotive air conditioning system using R444A and R152a refrigerants as alternatives to R134a," Int. J. Refrig., vol. 106, pp. 396–406, 2019, doi: 10.1016/j.ijrefrig.2019.06.008.

[35] P. Saengsikhiao, J. Taweekun, K. Maliwan, and T. Theppaya, "Investigation and analysis of R463A as an alternative refrigerant to R404A with lower global warming potential," Int. J. Refrig., vol. 118, pp. 58–68, Oct. 2020, doi: 10.1016/j.ijrefrig.2020.04.016.

[36] Gas Servei, "Technical Data Sheet – R-513A," 2024. [Online]. Available: https://gas-servei.com

[37] Appliance Update, "The current price of R134A refrigerant: What you need to know," Mar. 2025. [Online]. Available: https://applianceupdate.com/what-is-the-price-of-r134a-refrigerant/

[38] HomeGuide, "How much does a home AC recharge or Freon refill cost? (2025)," 2025. [Online]. Available: https://homeguide.com/costs/ac-freon-cost-recharge-refill

[39] Refrigerant Depot, "Honeywell HFO-1234yf 10 lbs," 2017. [Online]. Available: https://www.refrigerantdepot.com/product/honeywell-hfo-1234yf-10-lbs-free-shipping-refrigerant-depot/. [Accessed: Oct. 2, 2025].

[40] BHL.co.uk, "A-Gas Solstice ZE R1234ZE refrigerant rental cylinder 14 kg," [Online]. Available: https://bhl.co.uk/a-gas-solstice-ze-r1234ze-refrigerant-rental-cylinder-14kg-hfoze014-w624279.html. [Accessed: Oct. 2, 2025].

[41] United Refrigeration Inc., "R-450A refrigerant 25 lb cylinder," Product Catalog, 2025. [Online]. Available: https://www.uri.com/refrigerants-and-chemicals/refrigerants/gases/r450a/25r450a-zid25R450A-product

[42] Refrigerant Boys, "R513A gas cylinder 10 kg (1/4 SAE valve)," Official Store, 2025. [Online]. Available: https://www.refrigerantboys.com/en/buy/refrigerant-fluids/r134a/bombola-con-10-kg-di-gas-r513a-valvola-1-4-sae

[43] Z. Zhu, K. Liang, Z. Li, H. Jiang, and Z. Meng, "Thermal–economic–environmental analysis on household refrigerator using a variable displacement compressor and low-GWP refrigerants," Int. J. Refrig., 2020, doi: 10.1016/j.ijrefrig.2020.12.009.

[44] Q. Chen, G. Yan, and J. Yu, "Performance analysis of an ejector enhanced refrigeration cycle with R290/R600a for application in domestic refrigerator/freezers," Appl. Therm.

Eng., vol. 120, pp. 581–592, Jul. 2017, doi: 10.1016/j.applthermaleng.2017.04.027.

[45] V. Voloshchuk, P. Gullo, E. Nikiforovich, and N. Buyak, "Simulation and exergy analysis of a refrigeration system using an open-source web-based interactive tool—Comparison of the conventional approach and a novel one for avoidable exergy destruction estimation," Applied Sciences, vol. 11, no. 23, p. 11535, Dec. 2021, doi: 10.3390/app112311535.

[46] E. Söylemez, "Energy and conventional exergy analysis of an integrated transcritical CO2 (R-744) refrigeration system," Energies, vol. 17, no. 2, p. 479, Jan. 2024, doi: 10.3390/en17020479.

[47] N. Solanki, A. Arora, and R. K. Singh, "A comprehensive energy, exergy, environmental, and economic analysis of dedicated mechanical subcooled vapor compression refrigeration system," J. Therm. Anal. Calorim., vol. 149, pp. 1141–1154, 2024, doi: 10.1007/s10973-023-12761-6.

[48] S. Sanaye and H. R. Malekmohammadi, "Thermal and economical optimization of air conditioning units with vapor compression refrigeration system," Appl. Therm. Eng., vol. 24, pp. 1807–1825, 2004.

[49] Carolina HVAC, "A2L refrigerant switch HVAC costs: Navigating the impact on your budget," Sep. 2024. [Online]. Available: https://www.carolina-hvac.com/post/a2l-refrigerant-switch-hvac-costs-budget-impact

[50] Bellomy IMS, "The shift to eco-friendly refrigerants and its impact on costs," 2025. [Online]. Available: https://bellomyims.com/the-shift-to-eco-friendly-refrigerants-and-its-impact-on-costs/

[51] M. Aminyavari, B. Najafi, A. Shirazi, and F. Rinaldi, "Exergetic, economic and environmental (3E) analyses, and multi-objective optimization of a CO2/NH3 cascade refrigeration system," Appl. Therm. Eng., vol. 65, no. 1–2, pp. 42–50, Apr. 2014.

[52] R. Roy and B. K. Mandal, "Energy, exergy and economic optimization of a two-stage refrigeration system using low-GWP alternative refrigerants for high-temperature lift applications," J. Braz. Soc. Mech. Sci. Eng., vol. 45, p. 403, 2023, doi: 10.1007/s40430-023-04320-9.

[53] J. Wang, Z. J. Zhai, Y. Jing, and C. Zhang, "Particle swarm optimization for redundant building cooling heating and power system," Appl. Energy, vol. 87, no. 12, pp. 3668–3679, Dec. 2010.

[54] A. Islam, K. Srinivasan, K. Thu, and B. B. Saha, "Assessment of total equivalent warming impact (TEWI) of supermarket refrigeration systems," Int. J. Hydrogen Energy, vol. 42, no. 43, pp. 26973–26983, Oct. 2017, doi: 10.1016/j.ijhydene.2017.07.035.

[55] P. Makhnatch, A. Mota-Babiloni, A. López-Belchí, and R. Khodabandeh, "R450A and R513A as lower GWP mixtures for high ambient temperature countries: Experimental comparison with R134a," Energy, vol. 166, pp. 223–235, Jan. 2019, doi: 10.1016/j.energy.2018.10.065.

[56] C. H. de Paula, W. M. Duarte, T. T. M. Rocha, R. N. de Oliveira, and A. A. T. Maia, "Optimal design and environmental, energy and exergy analysis of a vapor compression refrigeration system using R290, R1234yf, and R744 as alternatives to replace R134a," Int. J. Refrig., vol. 113, pp. 10–20, May 2020, doi: 10.1016/j.ijrefrig.2020.01.011.

[57] F. Botticella, F. de Rossi, A. W. Mauro, G. P. Vanoli, and L. Viscito, "Multi-criteria (thermodynamic, economic and environmental) analysis of possible design options for residential heating split systems working with low GWP refrigerants," Int. J. Refrig., vol. 87, pp. 131–153, Mar. 2018, doi: 10.1016/j.ijrefrig.2017.10.030.

[58] C. J. L. Hermes, "Refrigerant charge reduction in vapor compression refrigeration cycles via liquid-to-suction heat exchange," Int. J. Refrig., vol. 54, pp. 186–192, Jun. 2015, doi: 10.1016/j.ijrefrig.2014.12.014.

[59] C. K. Rice, "The effect of void fraction correlation and heat flux assumption on refrigerant charge inventory predictions," ASHRAE Trans., vol. 93, no. 1, pp. 341–367, 1987.

[60] K. E. Tøndel and E. Brendeng, "The effect of void fraction model on estimation of air conditioner system performance variables under a range of refrigerant charging conditions," Int. J. Refrig., vol. 29, no. 7, pp. 1191–1200, Nov. 2006, doi: 10.1016/j.ijrefrig.2006.01.006.

[61] International Electrotechnical Commission, IEC 60335-2-89:2019—Safety of household

and similar electrical appliances—Part 2-89: Particular requirements for commercial refrigerating appliances with an incorporated or remote refrigerant unit or compressor, 2019.

[62] Danfoss, "New charge limits for flammable refrigerants: Your questions answered," 2019. [Online]. Available: https://www.danfoss.com/en/about-danfoss/our-businesses/cooling/refrigerants-and-energy-efficiency/refrigerant-faq-iec/

[63] MSA Safety, "IEC increases charge limits for flammable refrigerants," 2023. [Online]. Available: https://blog.msasafety.com/iec-increases-charge-limits-for-flammable-refrigerants/

[64] K. Takizawa, A. Takahashi, K. Tokuhashi, S. Kondo, and A. Sekiya, "Flammability assessment of CH2=CFCF3: Comparison with fluoroalkenes and fluoroalkanes," J. Hazard. Mater., vol. 172, no. 2–3, pp. 1329–1338, Dec. 2009.

[65] ANSI/ASHRAE Standard 34-2019, Designation and Safety Classification of Refrigerants. Atlanta, GA: ASHRAE, 2019.

[66] M. O. McLinden, A. F. Kazakov, J. S. Brown, and P. A. Domanski, "A thermodynamic analysis of refrigerants: Possibilities and tradeoffs for low-GWP refrigerants," Int. J. Refrig., vol. 38, pp. 80–92, Feb. 2014.

[67] SAE International, "HFO-1234yf low GWP refrigerant HMIS property standards," SAE Standard J2773, 2017.

[68] Y. Zhang and X. Chen, "Experimental and theoretical analysis of the mildly flammable zone of R1234ze(E)," Int. J. Refrig., vol. 60, pp. 316–323, Dec. 2015.

[69] F. Liu, S. Y. Motta, and S. Garimella, "Risk assessment methodology for A2L refrigerant systems in commercial buildings," Int. J. Refrig., vol. 158, pp. 112–125, 2024.

[70] Air-Conditioning, Heating, and Refrigeration Institute, Safety guidelines for A2L refrigerant handling and installation, AHRI-2023-SG-001, 2023.

[71] Underwriters Laboratories, "UL 2075 Standard for gas and vapor detectors and sensors—Updated for A2L applications," UL Standard Revision 2022-GV-001, 2022.

[72] International Electrotechnical Commission, "IEC 60335-2-40 leak detection requirements for A2L systems," IEC TC 61 Report, 2023.

[73] International Organization for Standardization, "ISO 5149 refrigeration system ventilation requirements," ISO TC 86 Report, 2023.

[74] Building Services Research and Information Association (BSRIA), "Ventilation design guide for low-GWP refrigerants," Tech. Rep. TR-2023-VD-001, 2023.

[75] International Electrotechnical Commission, "IEC 60529 degrees of protection standards for A2L applications," IEC Technical Standard Update, 2023.

[76] International Organization for Standardization, ISO 5149-1:2023—Refrigerating systems and heat pumps—Safety and environmental requirements—Part 1: Basic requirements, definitions, classification and selection criteria, 2023.

[77] European Committee for Standardization, EN 378-1:2023—Refrigerating systems and heat pumps—Safety and environmental requirements—Part 1: Basic requirements, classification and selection criteria, 2023.

[78] American Society of Heating, Refrigerating and Air-Conditioning Engineers, ANSI/ASHRAE Standard 15-2022—Safety Standard for Refrigeration Systems, 2022.

[79] [Missing bibliographic details in the source selection.]

[80] A. Hamza and T. A. Khan, "Comparative performance of low-GWP refrigerants as substitutes for R134a in a vapor compression refrigeration system," Arab. J. Sci. Eng., vol. 45, pp. 5697–5712, Jul. 2020, doi: 10.1007/s13369-020-04525-3.

[81] I. Dincer and M. A. Rosen, Exergy: Energy, Environment and Sustainable Development. Amsterdam, The Netherlands: Elsevier, 2007.

[82] A. Bejan, Advanced Engineering Thermodynamics, 4th ed. Hoboken, NJ, USA: John Wiley & Sons, 2016.

[83] B. O. Bolaji and Z. Huan, "Ozone depletion and global warming: Case for the use of natural refrigerant—A review," Renew. Sustain. Energy Rev., vol. 18, pp. 49–54, Feb. 2013.

[84] Y. Qin, N. Li, H. Zhang, and B. Liu, "Energy and exergy analysis of a modified three-stage auto-cascade refrigeration cycle using low-GWP refrigerants for sustainable development," J. Therm. Anal. Calorim., vol. 148, no. 3, pp. 1149–1162, Feb. 2023.

[85] Y.-J. Wei and T. P. Teng, "Evaluating retrofitting and operational efficiency of automobile air conditioners using environmentally-friendly refrigerants," Appl. Therm. Eng., vol. 268, Art. no. 125874, 2025.

[86] A. S. Karakurt, U. Gunes, and Y. Ust, "Exergetic and economic analysis of subcooling and superheating effect on vapor compression refrigeration system," in Proc. ASME Power Conf., Charlotte, NC, USA, Jun. 26–30, 2016, Paper No. POWER2016-59492, doi: 10.1115/POWER2016-59492.

[87] A. H. Mosaffa and L. Garousi Farshi, "Exergoeconomic and environmental analyses of an air conditioning system using thermal energy storage," Appl. Energy, vol. 162, pp. 515–526, Jan. 2016, doi: 10.1016/j.apenergy.2015.10.122.

[88] C. H. de Paula, W. M. Duarte, T. T. M. Rocha, R. N. de Oliveira, R. de Paoli Mendes, and A. A. T. Maia, "Thermo-economic and environmental analysis of a small capacity vapor compression refrigeration system using R290, R1234yf, and R600a," Int. J. Refrig., vol. 118, pp. 250–260, Oct. 2020, doi: 10.1016/j.ijrefrig.2020.07.001.

[89] M. A. M. Díaz, C. H. Martín, and J. J. Sánchez, Simulation Tool to Assist the Selection, Design and Optimization of Refrigerator Equipment and Components. València, Spain: Universitat Politècnica de València, Instituto de Ingeniería Energética, 2010. [Online]. Available: http://www.imst-art.com